

University of Alberta

Developing experimental methods for identifying the
sites of action of intraspinal microstimulation

By

Breanne M. Christian

A thesis submitted to the Faculty of Graduate Studies and Research in
partial fulfillment of the requirements for the degree of

Master of Science

Department of Cell Biology

Fall 2011

Edmonton, Alberta

- *To my loving husband, Jonathan, who never ceases to make me smile, for his extraordinary patience and continual support throughout my graduate study. To my admirable parents, who have always challenged and encouraged me to realize my potential. To my brother, Derek, for being a great role model, teaching me to hold my own. Thank you, and I love you!*

Abstract

Intraspinal microstimulation (ISMS) is a novel electrical stimulation approach to restore standing and ambulation in people with spinal cord injury. The technique entails inserting an array of microwires into the lumbosacral enlargement of the spinal cord to activate neuronal networks that control locomotion. Additionally, ISMS can be utilized to investigate the organization of these networks. In the present study, experimental methodology was developed to map the distribution of ISMS-activated neurons using immunohistochemistry to label c-Fos, an activity-dependent marker. The influence on c-Fos expression of the following conditions was studied: decerebration, laminectomy, microwire implantation, and ISMS. Data revealed that microwire implantation and decerebration minimally influenced c-Fos, while a laminectomy substantially increased c-Fos expression. Furthermore, results indicated that it is vital to monitor stimulation and adjust stimulus amplitude throughout the duration of stimulation. Using these data, a protocol was established that would aid in mapping the ISMS activated neuronal networks.

Table of Contents

Introduction	1
1.1 Spinal Cord Injury	1
1.1.1 Pathology of Spinal Cord Injury.....	3
1.1.1.1 Primary Injury.....	3
1.1.1.2 Secondary Injury.....	4
1.1.1.2.1 Insult to Vasculature following SCI.....	5
1.1.1.2.2 Inflammatory Response after SCI	6
1.1.1.2.3 Neurochemical Responses to SCI.....	7
1.1.1.2.4 Cellular Changes after SCI.....	8
1.1.2 Current Interventions.....	10
1.1.2.1 Cellular Implantation Techniques	11
1.1.2.2 Molecular Regenerative Techniques	11
1.1.2.3 Rehabilitation/ Functional Electrical Stimulation	13
1.2 Intraspinal Microstimulation	15
1.2.1 Benefits of ISMS	16
1.2.2 Understanding the Mechanisms of Action of ISMS.....	18
1.3 Spinal Cord Circuitry.....	20
1.3.1 Descending Drive	21
1.3.2 Sensory Afferents	24
1.3.3 Interneuronal Connections.....	26
1.3.4 Motoneurons	28
1.3.5 Central Pattern Generator	30
1.4 Immediate Early Genes	32
1.4.1 c-Fos	33
1.5 Overall Summary.....	35
1.6 Hypotheses.....	35
Materials and Methods	37
2.1 Overview of Experimental Procedures.....	37
2.2 Experimental Groups.....	38
2.3 General Surgical Procedures	39
2.4 Positive Control Experiments.....	41
2.5 Surgical Procedures for ISMS Experiments.....	42
2.5.1 ISMS Array Insertion	42
2.5.2 Application of Intraspinal Microstimulation	43

2.6 Development of Spinal Cord Tissue Processing	44
2.6.1 Spinal Cord Tissue Preparation	44
2.6.2 Optimization of Immunohistochemical Protocol	44
2.6.3 Immunohistochemistry Protocol.....	47
2.7 Data Analysis.....	48
Results	52
3.1 Antigen Retrieval Techniques are Beneficial for Immunohistochemistry	52
3.2 Effects of Surgical Preparations on c-Fos Expression.....	56
3.2.1 Decerebration.....	56
3.2.2 Laminectomy	60
3.3 Effects of Acute ISMS Array Implantation	60
3.4 Effects of ISMS Stimulation.....	62
3.4.1 ISMS without Surveillance.....	62
3.4.2 ISMS with Surveillance	66
3.5 Summary of Results.....	70
Discussion	71
4.1 Antigen Retrieval Techniques	71
4.2 Experimental Conditions	73
4.2.1 Decerebration.....	73
4.2.2 Laminectomy	75
4.2.3 Microwire Implantation.....	75
4.2.4 ISMS	76
4.3 Mapping Studies	77
4.3.1 Central Pattern Generator	77
4.3.2 c-Fos Mapping Studies	78
4.3.3 Understanding the mechanisms of action of ISMS	79
4.4 Limitations.....	80
4.4.1 Limitations of c-Fos Immunohistochemistry	80
4.5 Suggestions for Future Experiments.....	81
4.6 Conclusions	83
Bibliography	84

List of Tables

Table 1. Sensory Afferents	25
Table 2. Inhibitory Interneurons	28
Table 3. Experimental Groups	41

List of Figures

Figure 1. Intraspinal Microstimulation Array Implant	17
Figure 2. Rexed Laminae.....	21
Figure 3. Location of Descending Tracts in Spinal Cord	23
Figure 4. c-Fos Pathway	34
Figure 5. Surgical Timelines	41
Figure 6. c-Fos Positive Neurons	50
Figure 7. Antigen Retrieval with Proteinase K.....	54
Figure 8. Results of Antigen Retrieval	54
Figure 9. c-Fos in Motoneurons	55
Figure 10. Neuronal Distribution.....	57
Figure 11. Naïve Control	58
Figure 12. Decerebrate Controls.....	59
Figure 13. Decerebrate-with-Laminectomy Controls.....	61
Figure 14. Images of the Effect of Microwire Insertion.....	63
Figure 15. Effect of Microwire Insertion.....	64
Figure 16. Sham ISMS Controls.....	65
Figure 17. Comparison of Control Groups.....	65

Figure 18. Extensor ISMS without Surveillance67

Figure 19. Effect of Hemorrhaging in the Spinal Cord69

Figure 20. Extensor ISMS with Surveillance69

List of Abbreviations

AMPA	a-amino-3-hydroxy-5-methyl-4-isoxazolepropionic acid
AP-1	Activator Protein
CPG	Central Pattern Generator
DNA	Deoxyribonucleic Acid
FES	Functional Electrical Stimulation
HDAC	Histone Deacetylase
IEG	Immediate Early Genes
IHC	Immunohistochemistry
ISMS	Intraspinal Microstimulation
MK-801	(+)-5-methyl-10,11-dihydro-5H-dibenzo[a,d]cyclohepten-5,10-imine maléate
MLR	Mesencephalic Locomotor Region
mRNA	Messenger Ribonucleic Acid
NBQX	2,3-dihydroxy-6-nitro-7-sulfamoyl-benzo[f]quinoxaline-2,3-dione
NMDA	N-Methyl-D-aspartic acid
NMJ	Neuromuscular Junction
PBS	Phosphate Buffered Saline
Rb	Retinoblastoma Protein
SCI	Spinal Cord Injury

1. Introduction

1.1 Spinal Cord Injury

“I recall someone asking me how paraplegics had lived up to that time [prior to WWII]. The answer was, except in extremely rare cases, they usually died -- their life expectancy in those days was often less than a year. They got terrible bedsores, developed kidney and bladder problems, and simply lay in bed, waiting for death.”

- Dr. Howard A. Rusk, rehabilitation pioneer (Lanska, 2009)

During World War I, 80% of soldiers with spinal cord injury (SCI) died within two weeks due to complications of urinary tract infections and pressure ulcers. The few who survived had only partial spinal cord damage, retaining some sensory and motor function; however, rehabilitative strategies for these individuals were poor (Lanska, 2009). As clinical care for people with SCI and the management of the associated complications progressed, the average life expectancy for these individuals increased immensely. Currently, the average age to receive a SCI is 40.2 years old (University of Alabama at Birmingham, 2010). The spinal level and severity of damage affects an individual's life expectancy following SCI. The life expectancy for a person with paraplegia is 27.9 years post-injury. For an individual with tetraplegia, the life expectancy is 20.8 years

post-injury, but is further reduced to 12.2 years for ventilator-dependent individuals (University of Alabama at Birmingham, 2010).

The Christopher and Dana Reeve Foundation's paralysis resource center reports that there are currently 1,275,000 people living with a SCI in the United States (Christopher and Dana Reeve Foundation, 2009). The incidence of SCI is distributed in a gender and age-dependent manner, with the majority of cases occurring among men (van den Berg et al., 2010). The leading causes of SCI are motor vehicle accidents among young adults, and falls among the elderly population (Pickett et al., 2006). Sport-related injuries and gunshot wounds are less common, but may also result in a SCI (Christopher and Dana Reeve Foundation, 2009).

The ramifications of SCI are devastating for both the individual and his or her family members because of the person's dependence on others for performing daily tasks. Following SCI, other functional issues arise in addition to the loss of mobility. Insult to the spinal cord can also affect sexual, cardiac, bladder/bowel, respiratory, and thermoregulatory functions (Blight, 2002). However, paralysis is not only physically debilitating. SCI may also affect mental wellness (Elliott and Frank, 1996) and create impedances to social health (Noreau and Fougereyrollas, 2000), resulting in a reduced quality of life compared to non-disabled individuals (Dickers, 1997).

Although scientific investigations have substantially extended knowledge of the central nervous system and SCI, many obstacles remain to be overcome before successful spinal cord regeneration and repair are viable options (for review see

Blight, 2002; Amador and Guest, 2005; Thuret et al., 2006). Therefore, many researchers strive to improve the quality of life and decrease risks resulting from secondary conditions for people with SCI. Some researchers have specifically focused on implementing rehabilitative techniques, such as treadmill training and utilizing electrical stimulation to improve function, reduce spasticity, or regain muscle strength (Colombo et al., 2000; Edgerton et al., 2006).

The introduction of this thesis reviews the pathology and progression of SCI, followed by an examination of the current approaches to spinal cord repair and rehabilitation. The discussion of rehabilitation strategies focuses on the method of functional electrical stimulation, including intraspinal microstimulation (ISMS). The history and benefits of ISMS, which is currently under development to restore stepping and standing for individuals with SCI, is discussed. Spinal cord circuitry is described, as the ISMS technique may be a useful tool for understanding the organization of locomotor networks. The introduction concludes by demonstrating that immunohistochemistry is a useful approach for identifying ISMS-activated neurons.

1.1.1 Pathology of Spinal Cord Injury

1.1.1.1 Primary Injury

Neurological impairment after SCI occurs in two stages, namely primary and secondary injury. Primary injury occurs following forcible hyperextension/flexion or over rotation of the spinal column, which causes disc dislocations/ruptures or bone fractures (Dumont et al., 2001). There are four

classifications of SCI based on gross anatomical damage: compression, contusion/cavity, laceration, and solid cord injury (Bunge et al., 1993). Immediately following SCI, mechanical and vascular damage accumulates within the tissue (Norenberg et al., 2004). Insult to the vasculature and disruption of the blood-spinal cord barrier results in hemorrhaging and vasodilation that are initially localized in the grey matter of the spinal cord. It is presumed that this is due to the increased vasculature and a lower viscosity of the grey matter compared to the white matter (Gillilan, 1958; Wolman, 1965). The effects of damaged vasculature on neuronal death are discussed within secondary injury.

Unfortunately, clinicians have been unable to implement therapeutic interventions targeting the primary injury, as the time between receipt of SCI and effective medical attention is limited. It is suggested that the grey matter is beyond repair within one hour following the trauma, while damage in the white matter is irreversible after 72 hours post-injury (Blight and Young, 1989). One treatment that has been tested extensively in animal and human trials is the administration of methylprednisolone. The objective is to deliver the anti-inflammatory drug during the primary stage of injury to deter accumulation of secondary damage (Blight, 2002). However, the neuroprotective effects have remained controversial and serious side effects have been observed (for review see Amador and Guest, 2005).

1.1.1.2 Secondary Injury

Secondary injury is the damage that accumulates during later phases of SCI. Many therapeutic techniques have attempted to minimize secondary injury to

improve functional recovery for individuals with SCI (Mautes et al., 2000; Blight, 2002). The progressive expansion of injury is a result of chemical cascades, which include insult to the vascular system, influx of inflammatory cells, and activated neurochemical and cellular response mechanisms.

1.1.1.2.1 Insult to Vasculature following SCI

Trauma to the vascular system following SCI greatly disturbs normal blood flow and neuronal function. Mechanical damage of the vasculature results in hemorrhaging and ischemia, leading to additional damage of spinal cord tissue. Hemorrhaging is initially concentrated in the microvasculature of the grey matter, but intensifies and spreads over time (Tator and Fehlings, 1991; Mautes et al., 2000). The accumulation of blood in the spinal tissue places pressure on local neurons, leading to neuronal death (Liverman, 2005). Experimental results in a feline model with irreversible paraplegia generated from a weight drop contusion injury showed that the majority of vessels in the grey matter became hemorrhagic within an hour, while perfusion of the white matter progressively decreased for 8 hours, but returned to normal by 24 hours post-injury (Dohrmann et al., 1973). Subsequent to the progression of hemorrhaging, cavitation occurs at the lesion site and the region surrounding the injury becomes necrotic (Tator and Fehlings, 1991).

Ischemia, which is defined as inadequate blood flow, is a result of tissue compression, vasospasms, and the breakdown of the blood-spinal cord barrier (Mautes et al., 2000). Ischemia mainly impacts the white matter adjacent to the hemorrhaging grey matter (Tator and Fehlings, 1991) and was most substantial

around 24 hours in a rhesus monkey SCI model (Fried and Goodkin, 1971).

Degenerative mechanisms are triggered during ischemia and reperfusion of the spinal tissue, which are associated with the influx of toxic substances, such as free radicals. The abundant presence of free radicals results in neuronal death as they breakdown polysaturated fatty acid chains localized in cellular membranes (Mautes et al., 2000). For further explanation of the process of lipid peroxidation by free radicals see section 1.1.1.2.3 Neurochemical Responses to SCI.

1.1.1.2.2 Inflammatory Response after SCI

The inflammatory response following SCI plays a significant role in the progression of secondary damage. Two cell types involved in the inflammatory response are neutrophils and macrophages/microglia. Neutrophils are attracted to the lesion and surrounding necrotic zones by activated pro-inflammatory substances, such as interleukin-1 and tumor necrosis factor (Carlson et al., 1998). They infiltrate almost immediately, entering the damaged region of the spinal cord within the first hour after injury (Mautes et al., 2000). The concentration of neutrophils peaks at approximately 24 hours post-injury and reduces to 50% after two days (Dusart and Schwab, 1994). Comparably, macrophage recruitment is delayed. In a rat contusion injury model, very few macrophages were observed around 6 hours post-injury; however, they were abundant in the grey matter at 24 hours and peaked by 48 hours post-injury (Carlson et al., 1998). Initially, macrophages are converted from existing microglia, followed by an invasion of monocyte-derived macrophages (Mautes et al., 2000).

It is controversial whether the inflammatory response is predominately detrimental or beneficial for spinal tissue. Neutrophils and macrophages secrete free radicals and pro-inflammatory cytokines that initiate an inflammatory cascade and increase the extent of damage to the surrounding tissue (Norenberg et al., 2004; Liverman, 2005). However, microglia also provide neuroprotective benefits by releasing anti-inflammatory cytokines and neurotrophic growth factors that aid in tissue repair and neurite elongation (for review see Loane, 2010). Additionally, neutrophils and microglia remove debris by phagocytosis (Norenberg et al., 2004). Many therapeutic techniques aim to reduce the extent of secondary damage by blocking the influx of inflammatory cells; however, the benefits of these cells must also be considered (Loane, 2010).

1.1.1.2.3 Neurochemical Responses to SCI

Following SCI, reperfusion of ischemic spinal tissue, excessive release of the excitatory neurotransmitter glutamate, and an influx of calcium result in the production of free radicals (for review see Fiskum, 2000; Lewen et al., 2000). Over-activation of glutamate receptors results in calcium influx, which is accumulated within the mitochondria. High levels of intramitochondrial calcium promote production of reactive oxygen species through the mitochondria's electron transport chain (Fiskum, 2000). Ultimately, these reactive species promote further neuronal damage by exacerbating oxidative stress. Once stress levels exceed normal cellular antioxidant protective functions, free radicals dominate and oxidize cellular structures such as nucleic acids, proteins, and lipids, causing cell death (Lewen et al., 2000). Additionally, oxidative stress results in

the inactivation of cellular pathways (i.e. sodium-potassium ATPase, and mitochondrial respiratory enzymes) (Dumont et al., 2001).

The excessive release of glutamate also causes direct damage to the spinal cord (Dumont et al., 2001). The condition of the over-activation of glutamate receptors is termed excitotoxicity, which causes an influx of sodium, resulting in neuronal depolarization (Olney et al., 1971). However, following the inactivation of sodium-potassium ATPase activity, cell death occurs due to an accumulation of intracellular sodium (Choi, 1987). One strategy to reduce excitotoxicity is the application of glutamate receptor antagonists, such as MK-801 ((+)-5-methyl-10,11-dihydro-5H-dibenzo[a,d]cyclohepten-5,10-imine maléate) and NBQX (2,3-dihydroxy-6-nitro-7-sulfamoyl-benzo[f]quinoxaline-2,3-dione), which block NMDA (N-Methyl-D-aspartic acid) and AMPA (α-amino-3-hydroxy-5-methyl-4-isoxazolepropionic acid) receptors, respectively (Faden et al., 1988; Wrathall et al., 1996). However, systemic administration of these drugs could cause adverse side effects, such as short-term motor deficits or impact cardiorespiratory centers (Wrathall et al., 1996).

1.1.1.2.4 Cellular Changes after SCI

Neurons are exposed to an unstable environment following SCI due to pathophysiological changes. The two forms of cell death that occur are necrosis and apoptosis, which have several distinguishing characteristics. Necrosis is pathologically initiated by extreme environmental conditions, while apoptosis is initiated during normal physiological conditions (Fink and Cookson, 2005); however, apoptosis can also be initiated by external factors, such as inflammation

and free radical production that occur after SCI (Dumont et al., 2001). Necrotic cell death is characterized by nuclear decomposition and swelling that results in cell lysis, leading to an inflammatory response (Beattie et al., 2000). Comparably, apoptotic cells shrink in size and show membrane blebbing that leads to cellular fragmentation and the formation of apoptotic bodies (Beattie et al., 2000). Apoptosis is prevalent between 3 hours and 8 weeks post-SCI (Emery et al., 1998) and occurs among oligodendrocytes, microglia, and neurons (Shuman et al., 1997).

Axons transected by insult to the spinal cord are subject to Wallerian degeneration. The degenerative process entails the breakdown of the distal portion of a transected axon (Waller, 1850). An immunohistochemical silver staining technique has shown that the remaining portion of the axon swells and forms retraction balls near the transected end (Norenberg et al., 2004). A rat model with contusion injury has shown that spared neurons at the lesion site are subjected to chronic demyelination, resulting in reduction of conduction velocity (Totoiu and Keirstead, 2005). Spontaneous remyelination occurs beginning 7 days post-injury; however, it is unstable and incomplete (Totoiu and Keirstead, 2005).

Subsequent to neuronal degeneration, a glial scar is formed in the damaged spinal tissue (Norenberg et al., 2004). The majority of astrocytes that are located within the region of impact die. However, 2-3 weeks post-injury, astrocytes surrounding the lesion become hypertrophic and extend large, thick filaments, creating a scar that segregates the damaged region from viable tissue (Norenberg

et al., 2004). The astro-glia scarring not only generates a physical barrier that impedes regeneration of axons, but the astrocytes also secrete growth inhibitory molecules, such as proteoglycans, that repel axonal growth cones (Silver and Miller, 2004). Following a contusion injury in a rat model, excision of the glial scar, without affecting the surrounding neural tissue, resulted in significantly reduced locomotor recovery; however, functional recovery was not affected in a dorsal hemisection model (Rasouli et al., 2009). The study concluded that the role of the astro-glia scar, including structural and biochemical support, might differ based on the mechanism of injury (Rasouli et al., 2009). However, one variable in the study is the magnitude of injury from contusion relative to a controlled hemisection; therefore recovery in locomotor function may be based solely on the extent of injury.

1.1.2 Current Interventions

Many researchers are dedicated to developing treatments to improve the overall functional recovery for individuals with SCI. Studies have focused within various areas, which include 1) cell transplantation techniques to repair the neuronal circuitry by replacing dead neurons; 2) applying pharmacological agents to create a favorable environment for regeneration or reduce the extent of secondary damage; 3) rehabilitation to strengthen existing spinal cord networks, including the application of functional electrical stimulation (FES). Because of the complexity of SCI, substantial, successful functional recovery will most likely require a combination of the techniques listed above.

1.1.2.1 Cellular Implantation Techniques

Trauma to the spinal cord causes a severe loss of cells. Currently, numerous cell transplantation strategies are under development to improve regeneration of axons and restore function by replacing injured and dead cells. Implanted cells include Schwann cells, activated macrophages, embryonic and adult stem cells, and engineered stem cells (for review see Thuret et al., 2006). Adult stem cells have been obtained from various sources, including the dermis, spinal cord, bone marrow, and olfactory ensheathing cells (Thuret et al., 2006). Injections of bone marrow stromal cells and fetal stem cells have improved functional recovery of locomotion in rat SCI models (Zompa et al., 1997; Chopp et al., 2000). However, one residual challenge is to encourage stem cells to differentiate properly and integrate into the native tissue (Boulenguez and Vinay, 2009). Other bioengineering strategies have recently been developed utilizing materials, such as collagen, polymers, and silicone, to create a physical bridge to allow for axonal attachment (for review see Nomura et al., 2006). The insertion of these materials can be implemented in conjunction with cellular transplantation strategies (Nomura et al., 2006).

1.1.2.2 Molecular Regenerative Techniques

It is well known that injured axons in the peripheral nervous system are able to re-grow long distances, while spontaneous axonal regeneration is limited in the central nervous system (Aguayo et al., 1981). A study utilizing a sciatic nerve graft connecting the medulla and spinal cord showed that central axons can regenerate into the peripheral nerve following crush injury of the sciatic nerve

(David and Aguayo, 1985). However, regeneration within the central nervous system is limited due to the interactions between damaged central neurons and their environment (Aguayo et al., 1981), which is attributed to the absence of growth promoting molecules and the presence of inhibitory molecules that originate within the glial scar and oligodendrocytes (Fawcett, 2006).

Some therapeutic interventions focus on counteracting the inhibition of regeneration. For example, the administration of growth factors, such as brain derived neurotrophic factor, which promote axonal growth and neuronal survival, has been tested. Following insertion of gelfoam grafts consisting of growth factor-producing fibroblasts into the lesion site of a rat SCI model, results showed that axons regenerated or sprouted through the graft, significantly improving functional recovery (Murray et al., 2002). However, the technique is more beneficial during the acute phase of SCI, as axonal regeneration was limited following administration of growth factors in a chronic SCI rat model (Tobias et al., 2003). Therapeutic approaches have also attempted to block growth inhibitory proteins, such as Rho and Nogo that retard neurite outgrowth. Following SCI in rat and mouse models, the intracellular GTPase Rho, which leads to apoptosis, is present within neurons, oligodendrocytes, and astrocytes; however, the enzyme C3-05 can reverse the activation of Rho, providing cellular protection (Dubreuil et al., 2003). The Rho antagonist, C3, has been shown to enhance axonal regeneration through the lesion site in rat retinal neurons (Lehmann et al., 1999). Application of antagonists for myelin-derived inhibitory

factors that limit axonal growth, such as Nogo, has also been shown to improve regeneration, resulting in improved functional recovery (Merkler et al., 2001).

Several therapeutic drugs, including Minocycline and Riluzole, have been evaluated for their ability to reduce secondary damage. Following weight-drop contusion injury in a rat model, the antibiotic, Minocycline, provided neuroprotection through anti-inflammatory mechanisms (Lee et al., 2003). Immediately after SCI, administration every 12 hours reduced secondary damage and improved functional recovery of the hind limbs (Lee et al., 2003). Additionally, Minocycline attenuates apoptosis and gliosis (Festoff et al., 2006) through inhibiting NMDA-induced excitotoxicity and microglial production (Tikka and Koistinaho, 2001). However as stated previously, microglial cells are also beneficial for neuroprotection. Riluzole is also a promising neuroprotective agent, as it currently increases survival time for patients with amyotrophic lateral sclerosis, a neurodegenerative disease of motoneurons (Miller et al., 2007). It is suggested that riluzole decreases neuronal death by inhibiting presynaptic glutamate release (Rothstein, 1996).

1.1.2.3 Rehabilitation/ Functional Electrical Stimulation

A recent survey was performed to gain a better understanding of which physiological function, if partially regained, would most improve living situations for people with SCI. Restoring walking was ranked first or second priority for 45.5% of people with paraplegia and for 28.3% of people with quadriplegia (Anderson, 2004). The restoration of locomotion improves physical health, which provides a wide range of benefits, including reducing spasticity, bone loss, and

bladder/bowel complications, as well as improving muscle properties and overall cardiovascular health (Thuret et al., 2006).

Many rehabilitative training techniques have been implemented for individuals with paraplegia, as physical activity provides quality of life benefits for people with SCI by reducing pain, stress, and risks for health complications (Ditor et al., 2003). These conditioning strategies include manual and robotic assisted training, as well as body weight supported treadmill training (Colombo et al., 2000; Hornby et al., 2005). However, the objective for many researchers is to enable people with SCI to walk unassisted overground. Therefore, researchers have focused on utilizing functional electrical stimulation (FES) to restore ambulation (Field-Fote et al., 2005). Within the SCI community, the FES technique has not only improved walking (Peckham and Knutson, 2005), but also restored functional hand movements (Wheeler and Peckham, 2009) and bladder function (Kutzenberger et al., 2005).

There are two, external and implanted, peripheral FES methods that have been clinically implemented to improve gait. External, or transcutaneous, FES systems utilize surface electrodes located over the motor-points of the major muscles in the lower limbs. The Parastep, which alternates stimulation of the quadriceps muscle and flexor withdrawal reflex muscles, is one such system (Brissot et al., 2000). The Parastep is able to improve gait; however, many individuals with SCI opt to only utilize the system for physical exercise and not for daily ambulatory tasks (Brissot et al., 2000). The preference is due to the high cardiovascular and muscular metabolic demands, as the FES system requires

strong, continuous contractions to sustain stance (Brissot et al., 2000).

Implanted FES systems are more efficient, as electrodes are placed subcutaneously to directly stimulate muscle or nerves. The electrodes can be placed in several locations (i.e., intramuscular, epimysial, epineural, or cuffed around the nerve) (Peckham and Knutson, 2005). A study using multi-channel intramuscular stimulation demonstrated consistent, repeatable gait patterns for people with paraplegia (Kobetic et al., 1997). Implanted FES systems have also been implemented in conjunction with exoskeleton bracing for further stability (Kobetic et al., 2009). Although implanted systems are reliable, muscles remain highly fatigable, as target muscles are only partially recruited (Mushahwar et al., 2007). Therefore, another FES method, intraspinal microstimulation, is under development to resolve some of the issues with peripheral FES.

1.2 Intraspinal Microstimulation

A complete SCI at spinal level T6 or below results in paralysis of the lower limbs in the human; however, locomotor neuronal networks remain intact below the L1 spinal segment (Eidelberg et al., 1989). Intraspinal microstimulation (ISMS) utilizes the retained circuitry to generate functional movements. ISMS was previously utilized to restore bladder voiding following SCI (Nashold et al., 1971; Pikov et al., 2007). Currently, ISMS is under development to restore ambulation and the technique has previously demonstrated its ability to reanimate the lower limbs to produce stepping (Saigal et al., 2004) and standing (Lau et al., 2007) in the cat model.

In ISMS, an array of fine microwires (30 μ m diameter) is inserted into the lumbosacral enlargement, which is a 5-centimeter region in humans and 3 centimeters in the feline spinal cord [Figure 1]. The lumbosacral enlargement contains neuronal networks that are involved in controlling locomotion (Jankowska, 1992; Kiehn, 2006). The microwire tips are targeted to terminate in lamina IX within the ventral horn, which contains motoneuron pools that innervate specific muscles of the lower limbs (Vanderhorst and Holstege, 1997). Electrical pulses are transmitted through the microwires to activate spinal cord neuronal networks and ultimately, generate locomotor-like movements.

1.2.1 Benefits of ISMS

The ISMS technique has many clinical and functional benefits. In regards to the surgical implantation, ISMS is less invasive than implanted peripheral FES systems, as ISMS implants involve a small, compact region of the spinal cord (Prochazka et al., 2001). Moreover, laminectomy procedures to remove the spinous processes and expose the spinal cord are currently a common procedure in the operating room. The stimulating device remains stable as the spinal column provides support and protection for the implanted array (Prochazka et al., 2001). Furthermore, the presence of microwires causes minimal damage to the surrounding tissue. Chronic ISMS array implants in the rat spinal cord displayed encapsulation of the microwires; however, the implanted microwires did not reduce the adjacent neuronal density, nor affect cytoskeletal structures (Bamford et al., 2010). These findings were observed in sham control rats, as well as among rats stimulated 4 hours per day via ISMS for 30 days. The results show that

chronic administration of current to spinal tissue does not create additional damage (Bamford et al., 2010).

The direct stimulation of spinal cord networks using ISMS also has functional advantages over peripheral FES. Under normal physiological conditions, the smallest motoneurons are trans-synaptically activated first, recruiting fatigue-resistant fibers. Large, fatigable fibers are subsequently recruited for quick, large force production (Henneman and Olson, 1965).

However, applying electrical stimulation to motor axons during peripheral FES

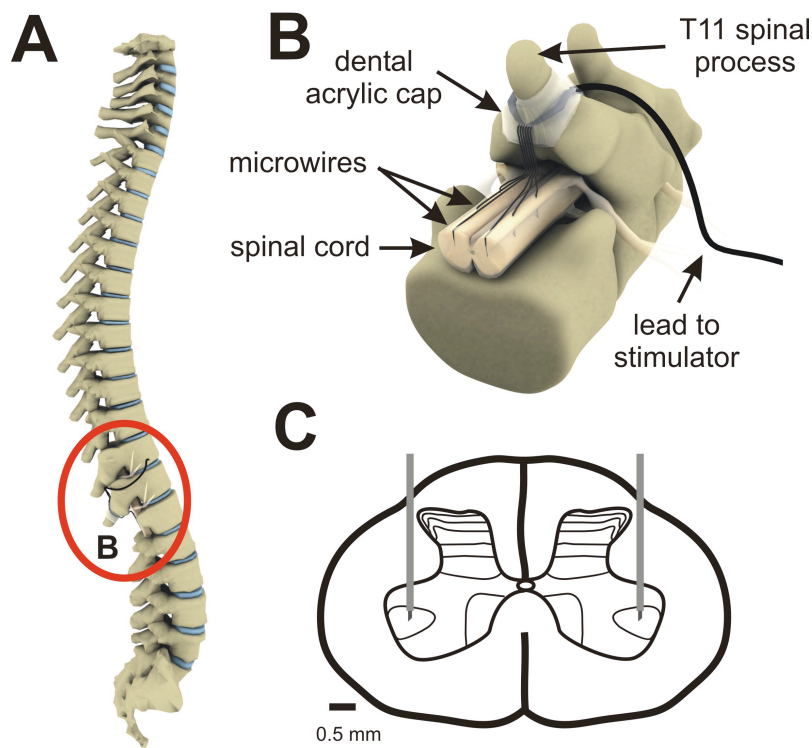


Figure 1. Intraspinal Microstimulation Array Implant. Cartoon illustration shows the anticipated intraspinal microstimulation (ISMS) implant for a human model. Reproduced from Guevremont (2007). **A)** The lumbosacral enlargement, enclosed with a circle, is the target for array implantation. **B)** ISMS microwires are inserted through the dorsal side of the spinal cord and are secured to the rostral spinous process with acrylic. **C)** Tips of microwires are located in the region of the motoneuron pools in lamina IX of the ventral horn gray matter.

results in recruitment of motor units in the reverse order, as the current selectively activates large motor units, resulting in steep force recruitment with small increases in stimulus intensity, followed by rapid force decay and fatigue (Singh et al., 2000). Comparisons have been made between intramuscular FES and ISMS-induced standing in the adult cat. With significantly lower levels of injected current than intramuscular stimulation, ISMS is capable of increasing the duration of standing due to a significantly reduced rate of force decay (Lau et al., 2007). The ability of ISMS to recruit fatigue-resistant fibers was demonstrated using immunohistochemical glycogen-depletion techniques (Bamford et al., 2005).

The production of lower limb movements with graded force recruitment curves suggests that ISMS activates motoneurons in a near-normal fashion, which enables the initial activation of fatigue-resistant fibers (Mushahwar and Horch, 2000). This further indicates that motoneurons are transynaptically activated through fibers in passage located around the microwire tips, resulting in a motoneuronal recruitment order similar to that seen with physiological activation (Gaunt et al., 2006; Calixto, 2007).

1.2.2 Understanding the Mechanisms of Action of ISMS

One would presume that electrically stimulating through a single microwire located in one motoneuron pool would only produce movement across a single joint. Instead, stimulation through an individual microwire can activate muscles across the hip, knee, and ankle joints, generating a full limb, flexor or extensor synergy (Saigal et al., 2004). Therefore, rhythmic bilateral stepping may be

produced by stimulating with as few as 4 microwires (two electrodes per limb). Although ISMS has demonstrated the ability to produce standing (Lau et al., 2007) and stepping (Saigal et al., 2004) in the feline model, the mechanism of action for ISMS is not entirely understood.

The microwire tips for ISMS terminate in the motoneuron pools located in lamina IX of the grey matter; however, stimulation in this region does not solely activate motoneurons. Lamina IX also contains fibers-in-passage (i.e. axons), as well as 7 times more interneurons than motoneurons (Mendell and Henneman, 1971). Therefore, the electrical current can activate any of these neuronal elements and spread both anti- and ortho-dromically to activate other neurons trans-synaptically. The fibers-in-passage include axons of sensory afferents (Gaunt et al., 2006), interneurons, and propriospinal interneurons (Calixto, 2007). Single cell recordings have previously shown that ISMS activates neurons in the immediate vicinity of the microwire tips, as well as neurons located rostrally and caudally up to several millimeters away (Calixto, 2007).

Previously, ISMS has been utilized to study motoneuronal and interneuronal synapses (Renshaw, 1940; Jankowska and Roberts, 1972). ISMS can also be used to gain knowledge of the organization of neuronal circuitry in the spinal cord. A great amount of research has been performed to understand the role of the central pattern generator (CPG), which is responsible for the intrinsic timing and rhythmic oscillations during walking (Brown, 1911); however, the exact location and configuration of the CPG is currently unknown (see section 1.3.5 Central Pattern Generator). Unique to ISMS, the technique is able to activate flexor and

extensor limb synergies separately. Therefore, ISMS may provide additional information regarding the CPG circuitry, which in turn, may improve ISMS proficiency, as well as treatments for the damaged circuitry following SCI.

1.3 Spinal Cord Circuitry

The spinal cord consists of a complex network of neurons that collectively work together to perform and modulate motor tasks. The white matter consists of ascending and descending axonal tracts that travel to and from the brain, as well as inter-segmentally within the spinal cord. The central gray matter contains cell bodies of interneurons and motoneurons, which receive input from dorsal, sensory afferents and subsequently relay information via the ventral roots to specific muscle groups.

Using histological techniques, the gray matter has been morphologically classified into regions, known as Rexed's laminae, which has become the standard nomenclature (Rexed, 1954). The dorsal horn contains laminae I-IV, the intermediate zone contains laminae V-VII, the ventral horn is comprised of laminae VIII and IX, and lamina X surrounds the central canal [Figure 2] (Rexed, 1954). Axonal projections to and from these laminae and their neuronal functions will be discussed below. It is important to understand circuitry within the spinal cord so that regenerative and rehabilitative techniques can be improved for individuals with SCI, as well as with other neurodegenerative diseases.

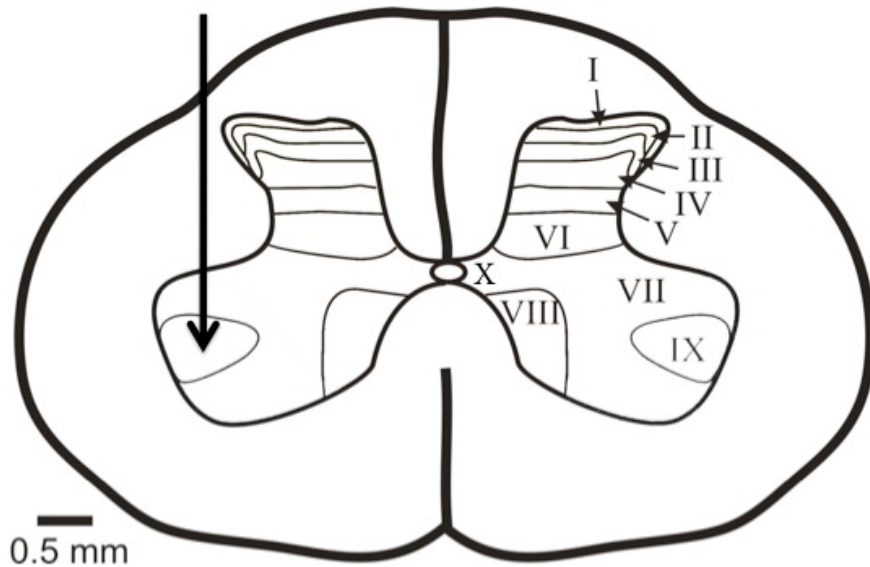


Figure 2. Rexed Laminae. Schematic diagram of the distribution of Rexed's laminae in the grey matter of a spinal cord cross-section. Arrow represents target location for ISMS microwires. Image adapted from (Guevremont, 2007).

1.3.1 Descending Drive

There are five descending tracts, originating from the cortex and brainstem that relay information to the spinal cord. These pathways are the corticospinal, vestibulospinal, reticulospinal, tectospinal, and rubrospinal tracts [Figure 3]. The corticospinal pathway is the strongest, most direct avenue for controlling muscles. These fibers originate in the motor cortex and terminate in the ventral horn of the spinal cord (Kandel et al., 1991). Approximately three-quarters of corticospinal axons cross contralaterally in the medulla at the pyramidal decussation, which form the lateral tract, while uncrossed fibers compose the ventral tract (Kandel et al., 1991). The majority of corticospinal axons synapse onto interneurons; however, some form monosynaptic connections with motoneurons (Kandel et al., 1991). The remaining tracts that originate in the brain stem are separated into medial and lateral pathways. The vestibulospinal, tectospinal, and reticulospinal

tracts compose the medial pathway and are responsible for postural control (Kandel et al., 1991). The lateral pathway is mainly comprised of the rubrospinal tract, which is involved in accomplishing goal-directed tasks (Kandel et al., 1991).

Additionally, there are descending tracts originating in the brain stem and hypothalamus that are involved in the initiation of locomotion, which include axons of neurons that utilize glutamate, dopamine, noradrenaline, and serotonin as neurotransmitters (Jordan et al., 2008). Activation of these pathways through the application of pharmacological agents to the brain stem or spinal cord elicits locomotor-like movements, which is a commonly utilized method to understand the distribution of locomotor neuronal networks in the spinal cord (See section 1.3.5 Central Pattern Generator, for review see Kiehn, 2006).

Along with the input from these descending pathways, there are other centers, such as the cerebellum, basal ganglia, and mesencephalic locomotor region (MLR) that are also involved in the control of locomotion. The cerebellum, which projects to regions in the brainstem, is able to modulate descending information to influence coordination and posture (Kandel et al., 1991). The basal ganglia and MLR direct their input through the reticulospinal tract, which is a critical component in the generation of rhythm during locomotion (Soffe et al., 2009). Electrical stimulation of the MLR, located in the brain stem, in a decerebrate cat preparation is able to induce locomotion (Jordan, 1998). However, it is suggested that the MLR is not necessary for the initiation of walking, nor for the performance of locomotion, as cats are still able

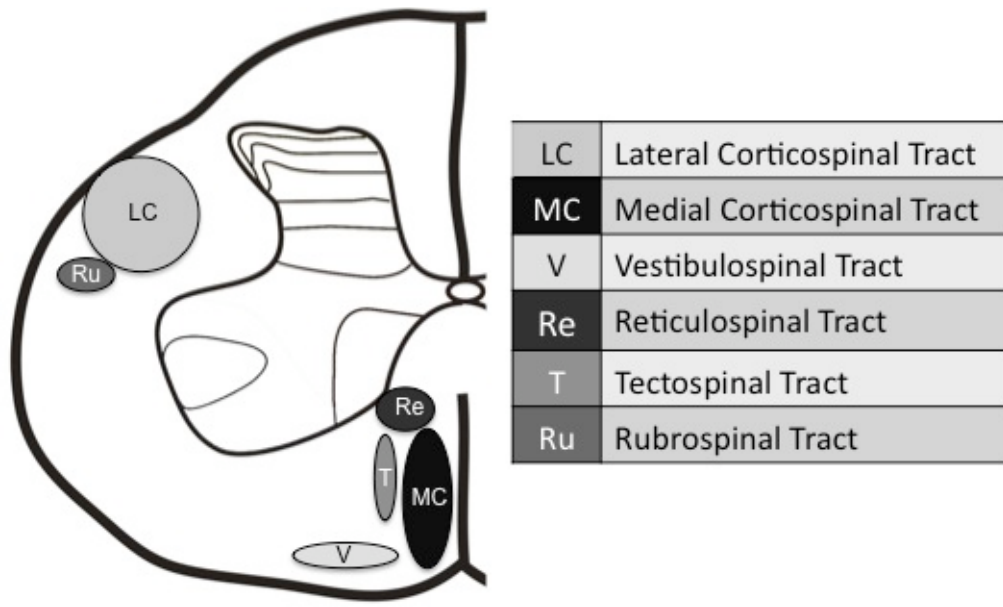


Figure 3. Location of Descending Tracts in Spinal Cord. Schematic drawing of half of a spinal cord cross-section. Filled ovals represent the general location within the spinal white matter of the five descending tracts originating in the cortex and brain stem.

to locomote after lesion of the MLR, although the hindlimbs are uncoordinated (Shik and Orlovsky, 1976). Recently, rhombencephalic neurons were discovered in the lamprey, which receive information from the MLR and project to the reticulospinal tract, amplifying glutamatergic excitation during locomotion (Smetana et al., 2010). The rhombencephalic neurons contain muscarinic receptors, which when blocked, retard mesencephalic stimulation-induced locomotion (Smetana et al., 2010). This pathway in the lamprey is analogous to the locomotor circuitry present in the brainstem that is described in vertebrates (Smetana et al., 2010).

Following complete spinal cord trans-section, all of these descending tracts are damaged and therefore, can no longer relay information to regions below the lesion site. After incomplete SCI, functional recovery varies among individuals,

depending upon which descending tracts are damaged. For instance, impairment of the corticospinal and rubrospinal tracts results in a greater extent of functional deficit (Raineteau and Schwab, 2001). Interestingly, the rubrospinal tract is capable of compensating for severe impairment of the corticospinal tract (Raineteau and Schwab, 2001). Functional recovery is limited and is attributed to the reorganization of descending pathways via sprouting or strengthening of existing synaptic connections at cortical and subcortical levels (Raineteau and Schwab, 2001). Another mechanism recently suggested as contributing to functional recovery of locomotion following SCI is the ability of serotonin receptors to become constitutively active, which relieves the spinal cord's dependence on receiving input from the serotonergic descending tract originating in the brain stem (Fouad et al., 2010).

1.3.2 Sensory Afferents

Sensory information, such as proprioception, pain, temperature, and touch, is relayed from muscles, joints, and skin to the spinal cord through afferent axonal projections, whose cell bodies are located in the dorsal root ganglia adjacent to the spinal cord (Kandel et al., 1991). For a summary of the sensory afferent fibers and their origination and termination sites, see Table 1. Cutaneous afferents are generally divided into unmyelinated C and myelinated A fiber classifications. The A fibers are further subdivided into $A\alpha$, $A\beta$, $A\gamma$, and $A\delta$ based on fiber diameter and conduction speed (Kandel et al., 1991). Lamina I and the dorsal portion of lamina II receive $A\delta$ sensory afferent input, which are the smallest myelinated fibers that transmit information regarding skin nociception (Rothwell,

1987). Neurons in lamina II are also the terminal endings for nociceptive, unmyelinated C fibers. Larger A α - A δ myelinated fibers terminate within laminae III and IV (Rothwell, 1987).

Table 1. Sensory Afferents. Table summarizes the categories of sensory afferent fibers and the type of information they provide to the spinal cord, as well as their sites of origin and termination.

Sensory Afferent	Fibers	Origin	Termination	Information Provided
Cutaneous	C	Skin	II	Unmyelinated, nociception
	A α	Skin	III, IV	Myelinated, nociception
	A β	Skin	III, IV	Myelinated, nociception
	A γ	Skin	III, IV	Myelinated, nociception
	A δ	Skin	I-IV	Myelinated, nociception
Group I	Ia	Muscle spindle	VI, VII, IX	Muscle length & velocity of stretch
	Ib	Golgi tendon organ	V-VI	Muscle tension
Group II		Joint receptors & secondary muscle spindles	IV-VIII	Limb position

Nerve fibers that convey proprioceptive information are divided into group I and group II afferents based on fiber diameter, conduction speed, and location of origin (Rothwell, 1987). Proprioceptive information is imperative during locomotion, as it provides feedback regarding limb position and enables movements to be modulated appropriately. Group I sensory afferents are the largest, myelinated fibers and therefore, have the fastest conduction velocity (>80m/s in cats) (Rothwell, 1987). Group I consists of Ia and Ib fibers that originate in muscle spindles and Golgi tendon organ receptors, respectively. Ia afferents transmit information regarding changes in muscle length and velocity of

stretch, while Ib fibers signal changes in muscle tension (Kandel et al., 1991). Upon entering the spinal cord, a single Ia axon from an individual muscle sends ascending and descending fibers that form synapses with over 90% of homonymous motoneurons (Mendell and Henneman, 1971). Ia axons also send collaterals that synapse with heteronymous motoneuron pools (Mendell and Henneman, 1971). Along with forming synapses with motoneurons in lamina IX, muscle spindle axons terminate on laminae VI and VII interneurons (Rothwell, 1987). Ib axons also bifurcate in the spinal cord and send synaptic terminals into laminae V-VII (Rothwell, 1987). Together, muscle spindle and Golgi tendon organ afferents maintain appropriate, consistent position and tension of the limb.

Group II afferents, which terminate in laminae IV-VIII, are smaller in diameter than group I and originate from joint receptors and secondary muscle spindle endings (Jankowska, 1992). Studies show that applying electrical stimulation to group II fibers results in flexor excitation and extensor muscle inhibition, which is generally termed the flexor reflex (Rothwell, 1987). Assessments of onset latency demonstrated that these excitatory connections are disynaptic, while inhibitory inputs to motoneurons are trisynaptic (Lundberg et al., 1987). However, not all stimuli to the group II afferents result in a flexor reflex, as the reflex response is dependent upon the intensity and location of a stimulus (Rothwell, 1987).

1.3.3 Interneuronal Connections

The spinal cord contains an intricate network of convergent and divergent interneuronal connections within the gray matter. The integrative circuitry relays

information pertinent to modulating reflex activity and producing rhythmic, oscillatory patterns, known as the central pattern generator (see section 1.3.5 Central Pattern Generator) (Brown, 1911; Kandel et al., 1991). Proprioceptive input is transmitted by interneurons with short and long-axons that send dendritic branches in every direction, activating motoneurons located in multiple motoneuronal pools (Jankowska, 1992). Interneurons are classified as first order interneurons, which receive input from sensory afferents, or last order neurons that synapse onto motoneurons (for review see Jankowska, 1992).

There are three classes of inhibitory interneurons, including Ia, Ib, and Renshaw cells that synapse onto motoneurons [Figure 5]. Ia inhibitory interneurons receive excitatory stretch information from muscle spindles and are responsible for reciprocal inhibition, allowing for relaxation of the antagonist muscle (Kandel et al, 1991). Ib interneurons receive information from Golgi tendon organs, providing negative feedback to adjust muscle tension by regulating the appropriate intensity of inhibition placed onto motoneurons of the homonymous muscle. Additionally, other Ib interneurons provide positive feedback on extensor muscles during locomotion (Kandel et al, 1991). Lastly, Renshaw cells form a negative feedback loop with motoneurons to regulate and stabilize motoneuronal firing rates (Kandel et al, 1991).

Another class of interneurons is the commissural interneurons [Table 2], which are located in laminae VIII and partly in VII that connect the spinal hemispheres through collaterals that extend across the midline (Matsuyama et al., 2006). The majority of these interneurons have short axons that synapse with

contralateral pre-motor interneurons and motoneurons within the same spinal segment (Matsuyama et al., 2006). Additionally, there are commissural interneurons that extend intersegmental ascending and descending axons (Matsuyama et al., 2006). The commissural interneurons are vital for regulating inter-limb coordination during locomotion (Jankowska et al., 2005).

Table 2. Inhibitory Interneurons. Table summarizes the types and functions of interneurons present in the gray matter of the spinal cord.

Interneurons	Input	Function
Ia	Muscle spindle	Reciprocal inhibition
Ib	Golgi tendon organ	Regulate inhibition of motoneurons
Renshaw	Motoneurons	Regulate motoneuron firing rates
Commissural	Group I & II afferents	Regulate contralateral interneurons and motoneurons for inter-limb coordination

1.3.4 Motoneurons

Motoneurons are classified as either gamma or alpha motoneurons, which innervate extrafusal and intrafusal muscles, respectively (Kandel et al., 1991). Gamma motoneurons contribute to the control of locomotion by modulating the reactivity of muscle spindles, while alpha motoneurons innervate skeletal muscle and are responsible for muscular contractions during locomotion (Kandel et al., 1991). Within laminae IX of the spinal gray matter, motoneurons are arranged into elongated, longitudinal groupings according to the muscles that they innervate; these groupings are termed motoneuron pools (Romanes, 1964). The spinal cord is enlarged in the cervical and lumbosacral regions, as these areas

contain the motoneuron pools that activate muscles of the upper and lower limbs (Romanes, 1964). A detailed rostro-caudal, medio-lateral map of the organization of these motoneurons in the lumbosacral spinal cord was determined using horseradish peroxidase retrograde tracings injected into muscles of the lower limbs in the cat model (Vanderhorst and Holstege, 1997). General mapping of motoneuron pools in the human has also been performed (Sharrard, 1964).

Together, the alpha motoneuron, peripheral axon, and the muscle cells that the axon innervates make up a motor unit, which generates functional voluntary actions (Kandel et al., 1991). The different characteristics of motor units result in varying contractile properties of muscles. More specifically, the contraction speed and generated force differ between motor unit types (see Kandel et al., 1991). These motor units are classified as fast fatigable, fast fatigue-resistant, and slow fatigue-resistant. Fast muscles are pale in color and produce forceful contractions, while slow skeletal muscles are dark red in color, with less forceful contractions (Rothwell, 1987). Generally, fast fatigable fibers are innervated by larger diameter axons and slow fatigue-resistant fibers are innervated by smaller diameter axons (Kandel et al., 1991). During muscle contraction, these fibers are recruited in order from lowest to highest threshold for synaptic activation (Rothwell, 1987). Smaller neurons have a higher input resistance due to reduced surface area, which allows them to reach threshold and depolarize more quickly (Rothwell, 1987). Therefore, smaller, fatigue-resistant motor units are activated first, followed by the recruitment of larger, fast fatigue-resistant units and

subsequently, high force-producing, fast fatigable units. This concept is known as the size principle (Henneman and Olson, 1965).

It is well known that these muscle properties adapt to changes in exercise routines. For example, following 3 weeks of knee immobilization in the human, muscle strength and muscle fiber size are significantly reduced (Hortobagyi et al., 2000). Even within the short time period, a proportion of muscle fibers transitioned from slow fatigue-resistant to fast units (Hortobagyi et al., 2000). The lack of activity is an issue for individuals with spinal cord injury, as their muscles become atrophied, less forceful, and more quickly fatigable.

1.3.5 Central Pattern Generator

It was originally suggested that proprioceptive reflexes control the progression of hindlimbs during locomotion (Sherrington, 1910). However, Brown demonstrated that locomotor-like stepping could be generated following deafferentation and thoracic spinal cord trans-section, which led to the conclusion that neither proprioceptive information, nor descending cerebral input is necessary for the generation of rhythmic hindlimb movements (Brown, 1911). Therefore, it was proposed that the mechanism for phasing inter-limb coordination was centrally located within the lumbar spinal cord. Brown further postulated that the neuronal networks may be organized as flexor and extensor antagonistic half-centers balanced and driven by “fatigue” of the neural centers (Brown, 1911). The intrinsic spinal mechanism for the control of muscle patterns and timing was later termed as the central pattern generator (CPG) (Grillner and Wallen, 1985). The CPG has since been heavily investigated to determine the organization and

location of the neuronal circuitry.

The theoretical model of the organization of the CPG remains under debate. Some investigators believe that the neuronal network is contained within a localized region, while others are convinced the circuitry is distributed along the lumbosacral enlargement (for review see Kiehn, 2006). Experiments utilizing a partitioned rat spinal cord preparation demonstrated that serotonin/NMDA bath application to the rostral spinal segments produces rhythmic locomotor-like activity, while stimulation of caudal segments results in tonic activity. These results led to the conclusion that the oscillatory properties are located in the rostral segments (Cazalets et al., 1995). Conversely, Grillner and Zangger's work supports the rostro-caudal distributed CPG model. Results following transverse sectioning of the isolated cat spinal cord showed that caudal segments also generate rhythmicity (Grillner and Zangger, 1979). Conclusively, studies demonstrate that the CPG is distributed as an excitability gradient along the lumbosacral enlargement with the rostral portion containing a greater rhythmic capacity than caudal segments (Kiehn, 2006).

There are possible explanations for the differences between the capacities of rhythmicity among spinal segments. Results may vary between studies based on the concentration and types of stimulatory neurotransmitters utilized to activate the locomotor-like movements (Kiehn, 2006). Additionally, neurons responsible for hip flexion are rostrally localized, while neurons that innervate muscles utilized during knee extension are located further caudally (Berkowitz, 2001). When rostral segments are transected, hip flexion can no longer be initiated,

which is required during overground ambulation; therefore, oscillatory capabilities are removed (Kiehn, 2006). The organization of spinal locomotor networks have been further described using immunohistochemistry to label activated neurons.

1.4 Immediate Early Genes

Following a variety of extracellular stimuli (i.e. thermal, electrical, mechanical, and chemical), transcription of immediate early genes (IEG) are rapidly activated, resulting in the synthesis of new proteins (Morgan and Curran, 1991; Curran, 1992). Immunohistochemistry (IHC) is commonly utilized to visualize the protein products of IEGs, such as Arc, pERK, and c-Fos, that signify localized neuronal activity. Arc expression is localized in dendrites and provides information regarding synaptic plasticity and long-term potentiation during learning and memory processes (Plath et al., 2006). Immunohistochemistry (IHC) of the protein kinase, pERK, is beneficial for understanding central sensitization in spinal cord dorsal horn neurons (Gao and Ji, 2009). However, pERK is not an appropriate neuronal tag following sub-threshold electrical stimulation, such as ISMS, as noxious stimulation activating C-fibers is required for pERK expression (Ji et al., 1999). For purpose of the present study, which is to map ISMS-activated neurons, c-Fos is the activity-dependent marker utilized.

1.4.1 c-Fos

C-Fos is a derivative from the Fos family (i.e. c-Fos, FosB, FRA-1, and FRA-2) of transcription factors (Hoffman et al., 1993). Under normal, basal conditions, c-Fos is expressed at very low levels in most cell types (Morgan and Curran, 1991). It is proposed that following cellular stimulation, the influx of calcium leads to dephosphorylation of Rb (retinoblastoma protein), releasing the HDAC (histone deacetylase) repressor complex, which enables transcription [Figure 4] (Qiu and Ghosh, 2008). The c-fos mRNA (messenger ribonucleic acid) is translated in the cytoplasm to produce the protein, c-Fos, which requires Jun to be translocation back into the nucleus (Chida et al., 1999). Members of the Fos and Jun families (i.e. C-Jun, JunB, and JunD) heterodimerize through a leucine zipper, forming an AP-1 (activator protein) binding complex (Curran et al., 1984). The complex binds to the DNA (deoxyribonucleic acid) AP-1 binding domain, which activates late response genes that further regulate cellular processes (Kovacs, 1998). The c-Fos protein is localized within the nucleus, which is easy to detect with IHC and allows for identification of individual neurons (Sagar et al., 1988).

C-Fos IHC is a practical, analytical tool due to the time course of synthesis and breakdown compared to other Fos proteins. The presence of c-fos mRNA transcripts can be detected as early as 5 minutes following stimulation (Greenberg and Ziff, 1984). Activation levels significantly increase around 30 minutes and reach maximal expression at approximately 60 minutes post-stimulation (Curran and Morgan, 1987). Compared to other members of the Fos family, the c-Fos

protein has an extremely short half-life of around 2 hours (Kovacs, 1998).

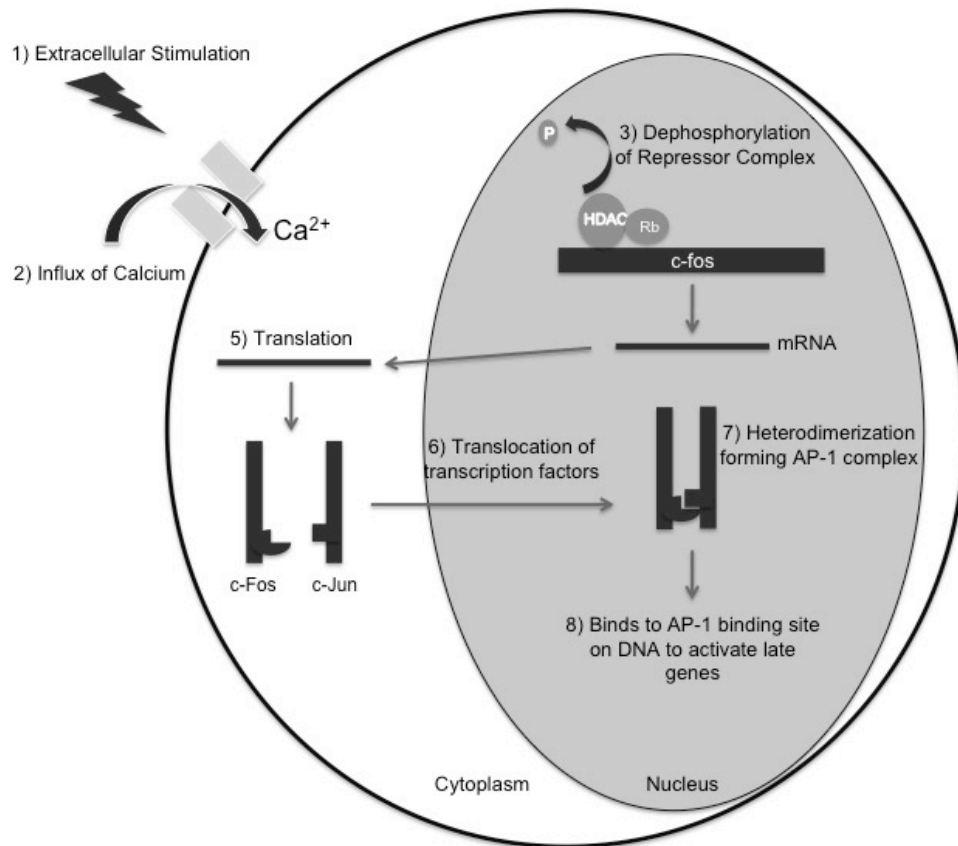


Figure 4. c-Fos Pathway. Diagram shows the pathway of c-Fos activation (Modified from Curran, 1992). Upon cellular stimulation, calcium-dependent transcription of the c-fos gene occurs. Following translation, c-Fos and c-Jun heterodimerize forming the AP-1 binding complex, which activates transcription of late genes. Abbreviations: Ca^{2+} - calcium; HDAC- histone deacetylase; Rb- retinoblastoma protein; P- phosphate; mRNA- messenger ribonucleic acid; AP-1- activator protein 1; DNA- deoxyribonucleic acid.

IHC of c-Fos has become a commonly utilized technique in neuroscience, as action potentials activate networks of c-Fos-positive neurons (for review see Kovacs, 1998). Specifically, c-Fos labeling has previously been used in the cat spinal cord to map regions of activity following electrical stimulation of peripheral nerves and the mesencephalic locomotor region (Dai et al., 2005; Gustafson et al., 2006). Therefore, the distributions of c-Fos-positive neurons

following ISMS can be compared to results from previous studies. C-Fos IHC only shows localization of general activity; however, more specific information on neuronal function can be obtained when combined with retrograde tracers and double labeling techniques (Krukoff, 1998).

1.5 Overall Summary

The introductory information presented in this thesis is the foundation of knowledge necessary for developing therapeutic interventions to improve functional recovery after SCI. It is important to not only understand the pathology of SCI and the factors that inhibit axonal regeneration and functional recovery, but additionally, the residual neuronal circuitry in the spinal cord that may be activated to restore function. While there are current FES methods utilized to restore ambulation for individuals with SCI, ISMS provides many benefits, such as a compact implant and reduced fatigue. The experimental methodology developed in the present study may be utilized to gain a better understanding of the mechanisms of action of ISMS and the organization of neuronal networks involved in locomotion.

1.6 Hypotheses

The overall goal of the study was to identify the neuronal networks activated by ISMS. Immunohistochemistry of c-Fos was utilized to locate and quantify the distribution of activated neurons. The initial hypotheses were as follows:

1) Neurons activated by ISMS collectively make up components of the inherent neuronal networks in the spinal cord that are involved in the control of locomotion.

2) Rostro-caudal distributions throughout the lumbosacral spinal cord will differ between flexor and extensor synergies.

Results from the experiments performed to answer the original hypotheses were disconcerting, as the data showed high background levels of c-Fos and similar levels of c-Fos expression for ISMS-stimulated and sham control animals. Therefore, the study focused on developing appropriate experimental methodology. The particular hypotheses tested were:

1) Animal surgical preparations (i.e. decerebration, laminectomy, and microwire array implantation) are confounding factors that can increase background levels of c-Fos expression.

2) Tonic ISMS, which is administered to produce a full limb synergy, may lose its effectiveness during the period of stimulation.

2. Materials and Methods

2.1 Overview of Experimental Procedures

The specific aim of the present study was to understand the influence of the experimental setup on c-Fos activation in the spinal cord. Therefore, the study was composed of several groups to investigate the influence of each surgical procedure. The experimental groups consisted of 1) positive controls, 2) control animals without ISMS implants (i.e. naïve, decerebrate, and decerebrate-with-laminectomy), and 3) animals with an ISMS array implanted in the lumbosacral enlargement of the spinal cord (i.e. sham ISMS and extensor ISMS with and without stimulation surveillance). C-Fos expression levels were compared for each of the experimental groups. Overall, the results aided in the development of a protocol appropriate for achieving the initial goal of mapping neuronal networks activated by ISMS.

A total number of 20 acute experiments were performed, consisting of eleven male adult cats (4.04- 5.74kg) and nine female adult cats (2.16- 5.12kg). Data were not analyzed from 5 animals due to experimental difficulties (i.e. hemorrhaging in the spinal cord or pre-mature termination of the experiment). All protocols for animal experiments were approved by the University of Alberta animal welfare committee and were in keeping with the standards of the Canadian Council on Animal Care.

2.2 Experimental Groups

The study initially consisted of three sets of experiments. 1) Positive control experiments (n=3) were conducted to activate widespread c-Fos expression in the spinal cord. The resulting tissue was utilized to optimize the immunohistochemical (IHC) protocol. 2) Extensor ISMS animals without stimulation surveillance (n=2) were performed to map the ISMS-activated neuronal networks. Electrical stimulation in the L6-L7 lumbar segments resulted in production of an extensor synergy. Mapping had previously revealed that this location produces specific multi-joint movements, or synergies, across the hip, knee, and ankle joints (Mushahwar et al., 2000). 3) Sham ISMS control animals (n=3) did not receive electrical stimulation and therefore, provided information on the effect of microwire implantation on c-Fos activation. Mapping of the ISMS-activated neuronal networks could not be obtained from ISMS and sham ISMS animals. Data revealed that there were confounding factors in the experimental protocol, resulting in elevated amounts of background, surgically-induced c-Fos.

Therefore, to understand the influence of the surgical preparations, additional experimental groups were included. 1) A naive control (n=1) established normal, basal levels of c-Fos expression in a healthy animal. 2) Decerebrate control animals (n=2) provided information on the effect of a decerebration. 3) Decerebrate-with-laminectomy controls (n=2) demonstrated the influence of a laminectomy on c-Fos activation. 4) Extensor ISMS with surveillance (n=2) ensured that the electrical stimulus was delivered appropriately

throughout the duration of stimulation. The stimulation amplitude was increased periodically, as necessary, to maintain a consistent, synergistic movement.

2.3 General Surgical Procedures

Immediately upon removal from the kennel, the naïve control animal was anesthetized with an intraperitoneal injection of sodium pentobarbital and intracardially perfused with a pre-wash solution (0.9% Saline, 100 units/mL Heparin) followed by 10% formalin (Fisher 10% Buffered Formalin Phosphate). The naïve control is excluded from the description below of the surgical procedure.

The remaining experimental groups were treated with the same initial surgical preparations. Animals were anesthetized with isoflurane gas and their bladders were evacuated. The right jugular vein was cannulated for drug administration and fluid maintenance throughout the duration of the surgery. Both carotid arteries were ligated and one was catheterized to monitor blood pressure. A tracheotomy was performed to allow for direct ventilation when needed. Following these surgical preparations, ISMS animals with surveillance were switched to sodium pentobarbital anesthetic for the remainder of the experiment. A laminectomy, removing L4-L6 spinous processes, was performed to expose the lumbosacral region of the spinal cord, except in decerebrate control animals. Warm saline was utilized to maintain spinal cord hydration. To stabilize the spinal cord, the animals were placed in a stereotaxic frame consisting of head, vertebral, and iliac crest clamps.

All animal preparations, excluding the ISMS extensor group with stimulation surveillance, received an inter-collicular decerebration, which entailed

removing the cerebrum by transecting the brain stem between the superior and inferior colliculi. The decerebration removed all sensory awareness, which allowed for the removal of anesthesia, as anesthesia depresses neural excitability and diminishes c-Fos expression (Jinks et al., 2002). Solu-medrol (2mL, 125mg methylprednisone sodium succinate) was administered to reduce any inflammation following decerebration. Dextran (1:2, Dextran 40: saline) was administered if necessary during the experiment to sustain appropriate blood pressure levels.

Following decerebration, there was a waiting period of 1 hour to allow the effects of anesthesia to dissipate. At this time, a neuromuscular junction (NMJ) blocker (gallamine triethiodide, 4 mg/kg/hr) was administered for the remainder of the experiment, except for positive control and extensor ISMS animals with surveillance. All animals remained untouched for an additional 3 hours to allow any surgically-induced c-Fos expression to degrade. The groups receiving stimulation were stimulated for the next 3 hours, while sham control animals with no applied stimulation waited for an additional 3 hours to maintain consistent timing across all experiments, totaling 7 hours of waiting post-decerebration for each animal. All experimental procedures were concluded with injection of sodium pentobarbital and an immediate intracardial perfusion. For a summary of the surgical procedures and timelines for the experimental groups, see Table 3 and Figure 5.

Table 3. Experimental Groups. Table summarizes the surgical preparations for each of the experimental groups.

Experiment	Decerebration	Laminectomy	Neuromuscular Junction Blocker	Stimulation
Naïve Control				
Positive Control	✓	✓		✓
Decerebrate Control	✓		✓	
Decerebrate w/ Laminectomy Control	✓	✓	✓	
Sham ISMS	✓	✓	✓	
Extensor ISMS w/o Surveillance	✓	✓	✓	✓
Extensor ISMS w/ Surveillance		✓		✓

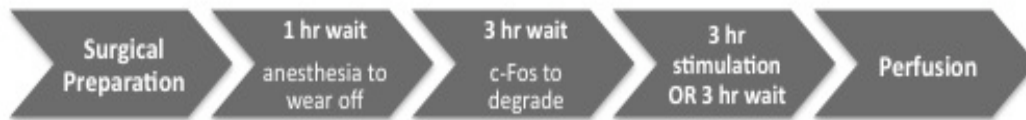


Figure 5. Surgical Timelines. Chart shows progression of experiments.

2.4 Positive Control Experiments

The purpose of conducting positive control experiments (n=3) was to utilize the tissue for optimization of the IHC protocol. These decerebrate animals received a L5-L6 laminectomy, followed by excision of the dura mater to expose the spinal cord. Activation of neurons, leading to c-Fos expression, was achieved through electrical stimulation via hook electrodes around the L6 dorsal roots on one side of the spinal cord, which generated a flexor withdrawal response of the corresponding hind limb. Stimulation was applied for 3 hours with 100ms bursts

of pulses delivered at a rate of 200 pulses per second, repeated every second. Stimulation amplitudes were increased accordingly to maintain consistent limb movements.

2.5 Surgical Procedures for ISMS Experiments

2.5.1 ISMS Array Insertion

A laminectomy was performed to remove the spinal dorsal processes and expose the lumbosacral region of the spinal cord for ISMS array implantation. A single test microwire was inserted in the spinal cord at various locations to determine the best site for array implantation that produced the desired movement. The ISMS microwire array was then implanted into the lumbosacral enlargement according to previously established techniques (Mushahwar et al., 2000). An array consisted of two rows of four, 30 μ m stainless steel microwires (California Fine Wire Company, Grover Beach, CA, USA) spaced 3 mm apart. Two of the sham ISMS control experiments used two rows of 6 microwires. The microwire tips were cut at a 15° angle, deinsulated approximately 60 μ m from the tip, and bent at a 90° angle. Approximately 4-4.5 mm of each microwire was inserted through the dorsal spinal cord targeting the motoneuron pools located in the ventral horns [Figure 1].

Once array implantation was complete, motor responses were visualized following stimulation through each microwire with multiple stimulus amplitudes. For the stimulation portion of the experiment, the electrical pulses were delivered through two ipsilateral microwires that produced optimal extensor synergies with

graded force. The sham ISMS control animals did not undergo stimulation and were not handled for the remainder of the experiment.

2.5.2 Application of Intraspinal Microstimulation

The extensor ISMS experimental groups received mono-polar stimulation for 3 hours at 25 pulses per second with stimulation interleaved between two microwires (200 μ s/phase; 1sec ON 9 sec OFF). Stimulus pulses were delivered as biphasic, charge-balanced pulses. Electrical stimulation was delivered only to one side of the spinal cord, which allowed for the contralateral side to be utilized as an internal control.

For the group without stimulation surveillance, constant stimulus amplitude was applied and fictive movements were achieved by administering a NMJ blocker (gallamine triethiodide, 4 mg/kg/hr). The drug was administered prior to stimulation to ensure that c-Fos expression was not induced by afferent feedback from contracting muscles. However, the paralyzing effects from the drug did not allow for monitoring and therefore, the evoked movements and modifications to the amplitude of ISMS could not be made.

The ISMS extensor group with stimulation surveillance did not receive the NMJ blocker, as movement of the stimulated hindlimb was necessary for monitoring, allowing for the stimulus amplitude to be adjusted throughout the stimulation. Animals in this group did not undergo a decerebration; therefore, sodium pentobarbital anesthetic was administered for the duration of the experiment. Although it is understood that the anesthetic would reduce c-Fos expression, the primary focus was to observe the output of the stimulation.

2.6 Development of Spinal Cord Tissue Processing

2.6.1 Spinal Cord Tissue Preparation

The lumbosacral enlargement was extracted from each animal and divided into spinal segments (L3-S1) based on the convergence of dorsal rootlets. The spinal cord tissue was post-fixed in 10% formalin at 4°C for 36 hours to maintain the localization of newly synthesized proteins. Following post-fixation, the spinal cord tissue was transferred to a cryoprotectant solution (30% sucrose in 0.1M PBS, pH 7.4) for approximately 2 weeks to remove water in the tissue and therefore, prevent crystallization. Each spinal cord segment (approximately 1 cm each in length) was individually wrapped in foil and frozen at -80°C for storage. The segments were then serially sliced into 20µm cross-sections using a cryostat (Leica Cryostat CM3050S) and mounted individually on slides (Superfrost Gold Plus, Fisher Scientific). Each slide was dipped in 95% ethanol to improve adhesion of the tissue to the slide by removing excess water. Slides were air-dried overnight and returned to the -80°C freezer. Prior to staining, the slides were removed from the freezer and set at room temperature for 30 minutes to allow the tissue to warm up.

2.6.2 Optimization of Immunohistochemical Protocol

Immunohistochemistry (IHC) is a widely used tool to identify proteins located in different cell populations. IHC techniques are continuously being developed to determine standard, reproducible protocols that provide optimal results for various immunostaining methods.

Fixation of tissue samples prior to IHC preserves the morphology of cellular structures. It is suggested that the “locked-in” state of proteins is achieved through methylene bridges that form cross-links between proteins (Montero, 2003). Although fixation is necessary to maintain the orientation of proteins, the cross-linking affects antibody penetration to the antigen (Otalı et al., 2009). Therefore, many IHC protocols utilize antigen retrieval techniques to counteract fixation and optimize the signal.

Antigen retrieval via proteolytic digestion has improved antigenicity by unmasking antigens in formalin-fixed tissue (Pileri et al., 1980); however, results have not been completely satisfactory, as proteolytic digestion is not advantageous for all antibodies (Pileri et al., 1997). Shi et al. demonstrated that heat-induced retrieval is superior at increasing antigen sensitivity than proteolytic enzymes (Shi et al., 1991). The advantages of heat-induced antigen retrieval techniques are reproducibility, improved signal-to-noise ratio, and the reduction of false negatives (Shi et al., 1997). Several solutions (i.e. water, citrate buffer, and saline) and methods for heating tissue (i.e. autoclave, microwave, and water bath) have been tested; however, the application of high temperature is the most important factor for improving retrieval (for review see Shi et al., 1997). Other factors that may provide different results between antibodies are pH, temperature, and length of time for heating. Therefore, it is important to test these conditions for each antibody (Shi et al., 1997). The most commonly used solution is citrate buffer (0.1M, pH 6.0) (Shi et al., 1995).

The present study compared antigen retrieval techniques (i.e. heating in citrate buffer and application of proteinase k) to determine the optimal method for improving antibody penetration. Incubation in proteinase k, causing proteolytic digestion, was deemed to be an inappropriate technique in conjunction with the primary antibody. Test trials were conducted to test the pH and temperature for heat-induced retrieval and confirmed that 0.1M citrate buffer (pH 6.0) at 85°C was optimal. Heating the tissue in citrate buffer successfully improved c-Fos visualization by amplifying the signal and increasing the number of c-Fos expressing neurons.

Additional trials were performed to further optimize the c-Fos IHC protocol. In the first trials, staining was localized in the cytoplasm of neurons, as opposed to being appropriately targeted in the nucleus. Therefore, the effects of tissue processing, such as length of fixation time (1-hour vs. 36 hour post-fixation) and freezing techniques (fast-freeze in 2-methylbutane vs. slow-freeze with tissue placed directly in the -80°C freezer) were compared, but were deemed to produce insignificant differences for protein visualization. A range of primary antibody (ab-5, PC38, Cedarlane) dilutions (1:500- 1:20,000) was evaluated; however cytoplasmic staining was still observed. The issue was ultimately resolved and nuclear staining was obtained after utilizing a c-Fos primary antibody from a different supplier (sc-52, Santa Cruz Biotechnology). The dilutions that were tested with the new antibody were 1:50-1:16,000.

Several blocking procedures were also tested to reduce background staining. Both incubation in hydrogen peroxide to block endogenous peroxidases and an

avidin/biotin-blocking step were deemed unnecessary. Comparisons were also made between a goat-serum blocker and a universal, serum-free blocking solution. Since results were similar, it was determined that the pre-fabricated universal blocker would maintain consistency across immunostaining trials. Based on these optimizing staining trials, the following protocol was developed and utilized throughout the study.

2.6.3 Immunohistochemistry Protocol

To improve antigen retrieval, slides were heated in 0.1M citrate buffer between 80-90°C for 20 minutes, followed by 20 minutes in citrate buffer at room temperature. The tissue was washed with phosphate buffered saline (PBS) and then enclosed with a hydrophobic barrier pen (H-4000, Vector Laboratories, Burlington, Ontario, Canada) to reduce the amount of solution needed per slide. A universal serum-free blocking solution (X0909, Dako) with 0.3% Triton X-100 was applied for 30 minutes to reduce non-specific, background staining. The primary antibody (1:800 rabbit polyclonal, sc-52 c-Fos, Santa Cruz Biotechnology) was then applied in PBS with 0.3% triton and the tissue incubated overnight at 4°C. The following day, the tissue was washed in PBS and incubated in the secondary antibody (1:200 biotinylated goat anti-rabbit, BA-1000, Vector Laboratories) for 1 hour. For signal amplification, the tissue was incubated for another hour in vectastain avidin and biotin (ABC) reagent (PK-6100, Vector Laboratories). A diaminobenzidine and nickel chloride substrate (SK-4100, Vector Laboratories) was used for visualization of the proteins. The tissue was then processed through a gradual dehydration in ethanol, followed by

xylene washes before being cover-slipped with a xylene-base mounting medium (Protocol 245-691, Fisher Scientific).

The IHC protocol was also utilized to obtain the distribution of neurons by substituting the primary (1:250 mouse monoclonal, A60 anti-neuron, Millipore) and secondary antibodies (1:200 biotinylated horse anti-mouse, Vector Laboratories) to label neuronal nuclei.

2.7 Data Analysis

Each spinal segment of the lumbosacral enlargement (L3-S1) was sliced in a repeated pattern of mounting 7 tissue sections on individual slides, followed by discarding a number of sections based on the length of the spinal segment (i.e. L3: skip 15; L4: skip 15; L5: skip 10; L6: skip 10; L7: skip 10; and S1: skip 5).

Within the groupings of 7 cross-sections, the first slide was stained for c-Fos (not for all groupings), while the remaining slides were kept for additional staining (i.e. neuN: neuronal nuclei) and as spare tissue. For each of the six spinal segments, ten evenly distributed tissue sections were immunostained for c-Fos, totaling 60 spinal cord sections per animal for analysis. The minimal distance between two analyzed cross-sections was 0.48 mm.

Images of the cross-sections were taken using a Leica microscope (Leica Microsystems, Wetzlar, Germany) with SPOT Software (SPOT Imaging Solutions, Sterling Heights, MI, USA). Adobe Photoshop was utilized to merge the images together to create a seamless image of the grey matter for each tissue section.

Quantification of c-Fos was performed manually; therefore, a set of inclusion criteria was determined. Cells determined to be c-Fos-positive neurons met the following criteria: 1) had a large, round nucleus; 2) the nucleus was completely stained; and 3) the nucleus was stained darker than the surrounding cytoplasm [Figure 6]. Cells excluded as c-Fos expressing neurons are described as follows: 1) cells were small in diameter or irregular in shape; 2) the nucleolus was stained noticeably darker than the nucleus; 3) the cytoplasm was stained darker than the nucleus; and 4) the nucleus was incompletely stained.

Manual counting of c-Fos expressing neurons in the grey matter of the spinal cord was divided into six bins, based on the laminar characterization previously determined by Rexed [Figure 2] (Rexed, 1954). The bins included: Laminae I-IV, V-VI, VII, VIII, IX, and X. These bins were divided based on the main function or input to neurons located in specific laminae (i.e. I-IV: cutaneous input; V-VI: group I & II afferents; VII: group II afferents & many interneuronal connections; VIII: commissural interneurons; and IX: motoneurons).

Data from the experimental groups were compared by laminar and segmental distributions of c-Fos. The laminar distribution, based on the 6 bins discussed above, described the localization of c-Fos positive neurons within the grey matter. The type and role of neurons can be classified based on their laminar location. The segmental distribution described the rostro-caudal extent of neuronal activation. For ISMS-stimulated animals, the distribution demonstrates the ability for the electrical current to travel to segments rostral and caudal of the implanted microwires to generate hindlimb synergies.

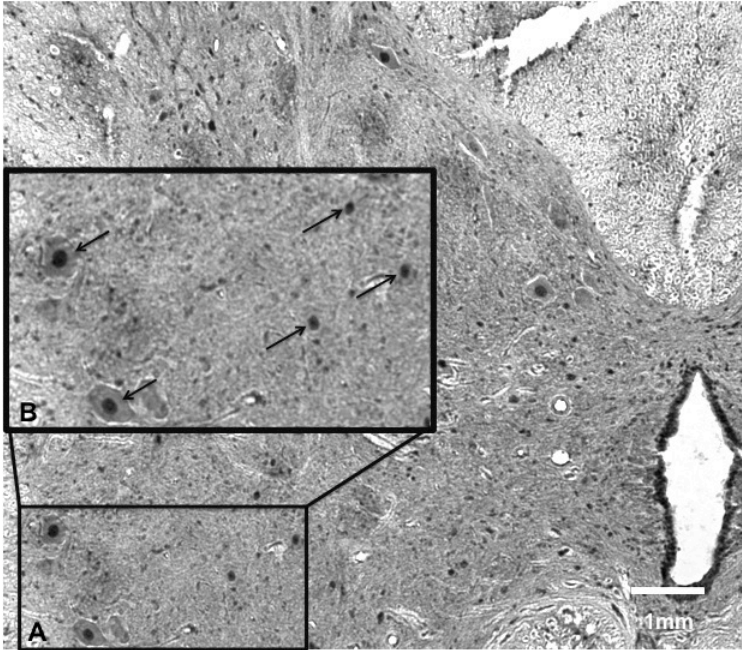


Figure 6. c-Fos Positive Neurons. Cat spinal cord tissue immunostained with the c-Fos antibody. Box B is an enlarged image of box A. Arrows clarify cells that met the inclusion criteria and were counted as c-Fos expressing neurons.

For ISMS preparations, stimulation was only applied to one side of the spinal cord, which allowed for the comparison of left and right hemi-sections. C-Fos expression for control animals was similar between left and right hemi-sections, as they received the same treatment; therefore, these two sides were averaged. When analyzing results across groups, the stimulated side of the spinal cord for ISMS preparations was compared to the average of left and right sides of the spinal cord for control animals. Therefore, the graphs in the results section represent the average number of c-Fos positive neurons present in one half of the spinal cord per spinal segment.

Results are represented as the mean number of c-Fos expressing neurons. For control groups, the mean was calculated by averaging 10 sections for each spinal segment, followed by averaging the means of the left and right hemispheres

then averaging again across the animals for each experimental group. Therefore, error bars in the graphs represent the standard error. For ISMS stimulated animals, the mean was determined by averaging 10 sections for each spinal segment for the stimulated side of the spinal cord, followed by averaging across animals in the ISMS group. Therefore, error bars again represent the standard error. In instances when graphs represent the distribution for a single ISMS animal, error bars represent the standard deviation across the 10 sections for the stimulated side of the spinal cord.

Statistics were not performed for any of the data, as the sample size for each of the groups was too small. For any study involving animals, a balance should be met between attaining information and the sample size. Originally, a sample size of 3 was selected as the minimum number of animals for each of the experimental groups that could provide reliable information. When the scope of the present study was shifted to developing experimental methodology, it was necessary to add several groups. Therefore, to limit the number of cats utilized for the project, the sample size was reduced to 2 animals per group. For the naïve control experiment (n=1), c-Fos expression levels were low as expected and therefore, no additional naïve experiments were performed. The sample sizes were a limitation in the study; however, trends between experimental groups were observed, allowing for the development of a protocol that could be utilized to answer the original hypotheses.

3. Results

The ISMS technique can potentially provide information on the localization of neuronal networks in the lumbosacral enlargement involved in locomotion. Previous studies have utilized activity-dependent markers, such as c-Fos, to map distributions of neurons in the cat spinal cord that are activated following peripheral and supraspinal stimulation (Dai et al., 2005; Gustafson et al., 2006). However, the immediate early gene, c-fos, is easily activated by a variety of stimuli, including surgical procedures. The goal of the present study was to develop appropriate experimental methodology to use c-Fos IHC following ISMS to investigate the organization of locomotor networks in the spinal cord.

3.1 Antigen Retrieval Techniques Are Beneficial for Immunohistochemistry

Antigen retrieval techniques increase antigenicity during IHC (Ino, 2003) (Shi et al., 1997). In the present study, antigen visualization following different antigen retrieval methods (i.e. proteolytic digestion, heat-induced retrieval, and no retrieval technique) was quantified and compared across serial tissue sections. The number of c-Fos positive neurons was calculated and averaged for 3-5 tissue sections from spinal segment L6 for each retrieval method. The treatments were compared for ISMS (n=1), sham ISMS control (n=1), and positive control (dorsal root stimulation) (n=1) experimental conditions. ISMS and positive control

animals received electrical stimulation in the L6 spinal segment. The sham ISMS control animal received microwire implantation in the L4 and L5 spinal segments.

The application of proteinase K for proteolytic digestion in the present study was not an appropriate antigen retrieval technique in combination with the c-Fos antibody, as c-Fos could not be visualized [Figure 7]. On the other hand, heat-induced retrieval via incubation in citrate buffer at 85°C was beneficial. Compared to non-treated tissue, citrate buffer heating substantially increased the counts of c-Fos-positive neurons; however, c-Fos visualization was not increased by the same factor for each of the experimental groups due to differences in stimulus conditions [Figure 8]. Following heat-induced retrieval, the positive control animal demonstrated substantially more c-Fos positive neurons than ISMS and sham ISMS animals relative to tissue immunostained without antigen retrieval [Figure 8].

Previous studies discussed the lack of c-Fos expression in motoneurons (Dai et al., 2005, Hunt et al., 1987, Dampney et al., 1995). However, observations from the present study demonstrated that utilization of the heat-induced antigen retrieval technique enables the visualization of c-Fos in motoneurons. For ISMS-stimulated spinal cord tissue treated with citrate buffer (average of 5 cross-sections) there was an average of 15 c-Fos-positive neurons located in lamina IX, while tissue immunostained without antigen retrieval (average of 4 cross-sections) had approximately 2 c-Fos expressing neurons in lamina IX [Figure 9].

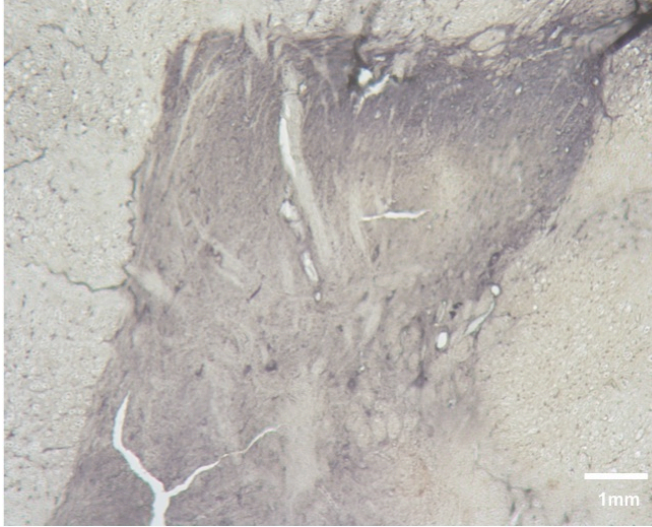


Figure 7. Antigen Retrieval with Proteinase K. Image is of the right dorsal horn of a cross-section of spinal cord tissue treated with proteinase K. The absence of c-Fos visualization demonstrated by the lack of black, punctate nuclei in the grey matter shows that the c-Fos IHC protocol utilized in the present study in conjunction with proteinase K antigen retrieval is ineffective.

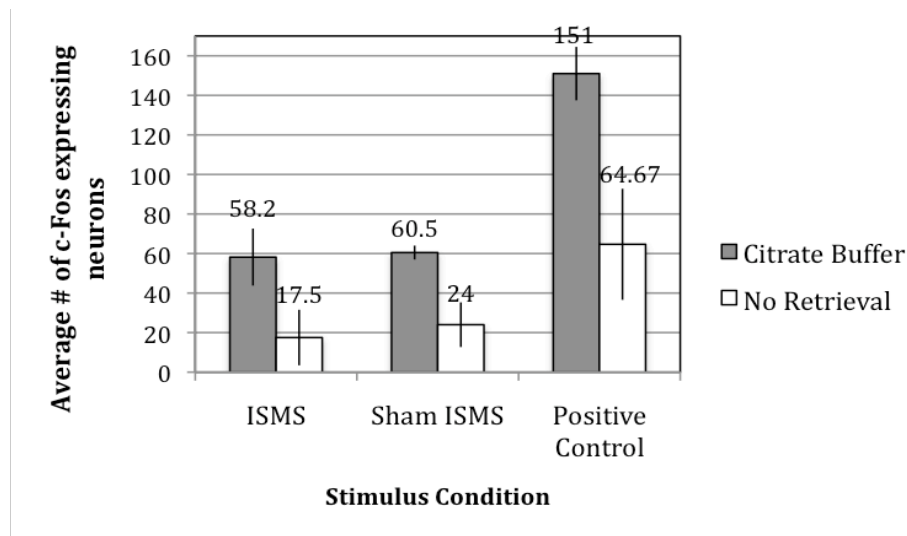


Figure 8. Results of Antigen Retrieval. Summary of the effect of antigen retrieval on c-Fos visualization is shown. The bars represent the mean \pm standard deviation of neurons expressing c-Fos (values above represent the mean) in the L6 spinal segment of the spinal cord following three stimulus conditions: ISMS, sham ISMS control, and positive control. The mean was calculated by averaging the number of c-Fos positive neurons on the stimulated side of the spinal cord over 3-5 tissue sections. Antigen retrieval substantially increased the visualization of c-Fos expressing neurons. Dorsal root stimulation (positive control) activated more neurons than ISMS and ISMS array implantation (sham ISMS).

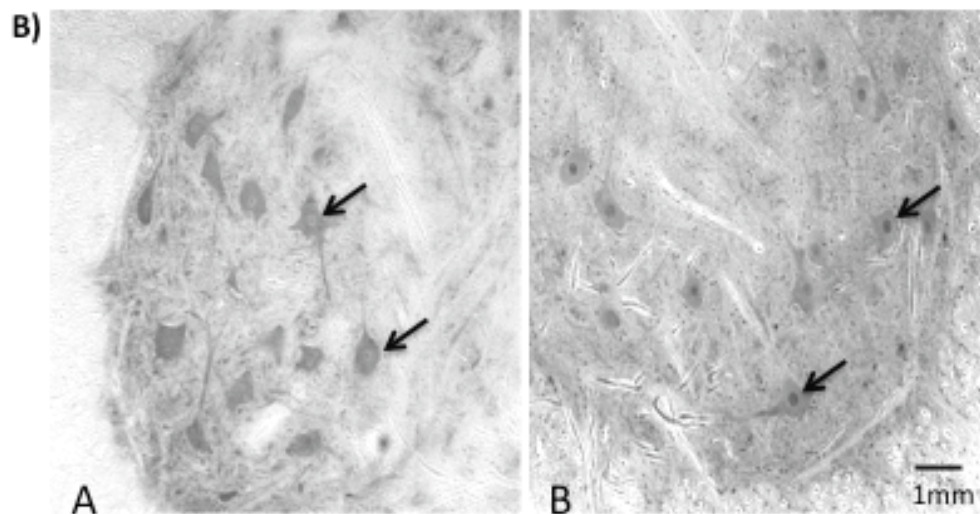
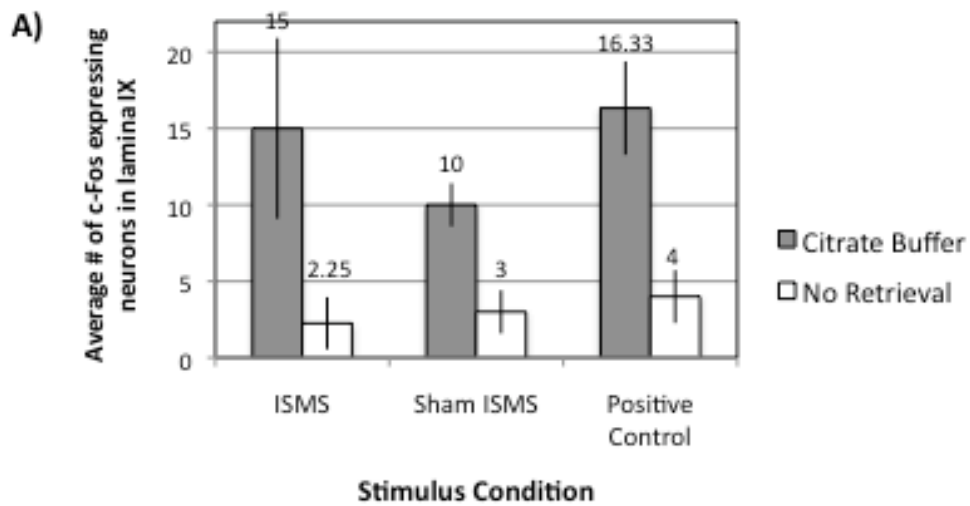


Figure 9. c-Fos in Motoneurons. A) The bar graph represents the mean \pm standard deviation of neurons expressing c-Fos located in lamina IX for the L6 spinal segment of the spinal cord for the following stimulus conditions: ISMS, sham ISMS, and positive control. The mean was calculated by averaging the number of c-Fos positive neurons in lamina IX on the stimulated side of the spinal cord for 3-5 tissue sections. The utilization of antigen retrieval substantially improved the visualization of c-Fos in motoneurons for all experimental groups. B) Images of c-Fos immunostaining in the ventral horn for consecutive slices of spinal cord tissue from the L6 spinal segment. A: Absence of c-Fos in tissue without application of an antigen retrieval treatment. B: Tissue heated in citrate buffer demonstrates the presence of c-Fos in motoneurons. Arrows draw attention to examples of motoneurons.

3.2 Effects of Surgical Preparations on c-Fos Expression

Under normal physiological conditions, c-Fos is expressed at low basal levels in most tissue types (Morgan and Curran, 1991). For the present study, the basal level of c-Fos expression was determined in a naive control, which was anesthetized and perfused immediately upon removal from the kennel. The results were normalized by dividing the total number of neurons present in a cross-section by the number of c-Fos expressing neurons. A neuron specific stain (neuN) was utilized to obtain the neuronal counts, which were averaged across 3 sections of spinal cord tissue per spinal segment (L3= 243, L4= 285, L5= 284, L6= 577, L7= 382, S1= 518) [Figure 10]. For all spinal segments in the lumbosacral enlargement (L3-S1), the percent of c-Fos expressing neurons normalized to the total number of neurons was 5% or less [Figure 11].

3.2.1 Decerebration

Decerebrate control experiments entailed an inter-collicular decerebration followed by 7 hours of waiting prior to perfusion to maintain consistent timing with other experimental groups. A NMJ blocker was administered following the one-hour post-decerebration time window that was allotted for the effects of the gas anesthetic to diminish; therefore, the presence of excitability (e.g. extensor rigidity) that occurs after a decerebration could not be observed beyond that time. Decerebrate spinal cord excitability was exhibited to varying intensities among animals in each of the experimental groups. For one decerebrate control animal, which demonstrated rhythmic movements in the tail prior to administration of the

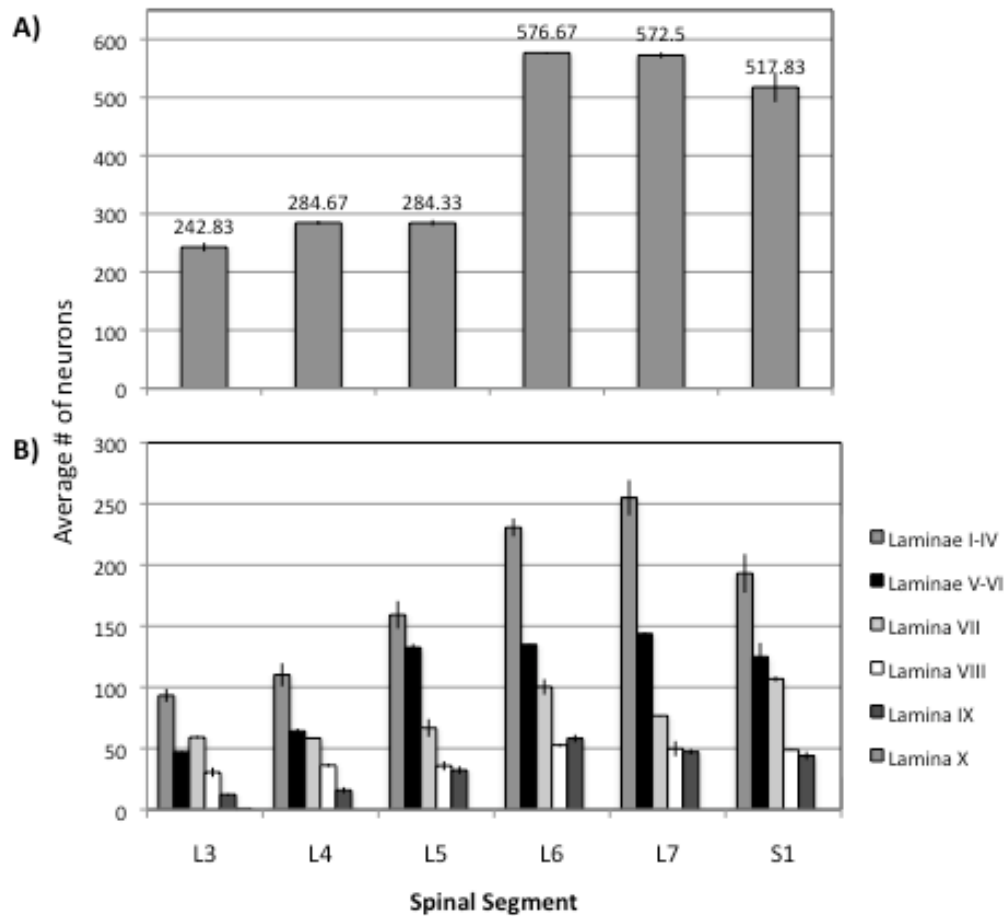


Figure 10. Neuronal Distribution. Shown is the mean \pm standard error of the total number of neurons present in each spinal segment. The mean was calculated by determining the average number of neurons on the left and right sides of the spinal cord for 3 tissue slices, followed by averaging the two sides for each spinal segment. **A)** Segmental distribution. **B)** Laminar distribution.

NMJ blocker, c-Fos expression levels were similar to those of the naive control.

However, the second decerebrate control did not indicate any signs of excitability during the hour, but showed elevated counts of c-Fos for L4 and L6-S1 spinal segments compared to the naive control animal [Figure 12]. Although, rigidity was not observed, it could have been present during the time of NMJ blocker administration. Differences between the decerebrate control animals were also

observed when comparing laminar distributions. The first animal demonstrated consistent, low levels of c-Fos for all laminae, while the second animal had peaks of c-Fos expression in laminae V-VII. The results show variability among animals due to the impact of decerebration on c-Fos expression in the spinal cord.

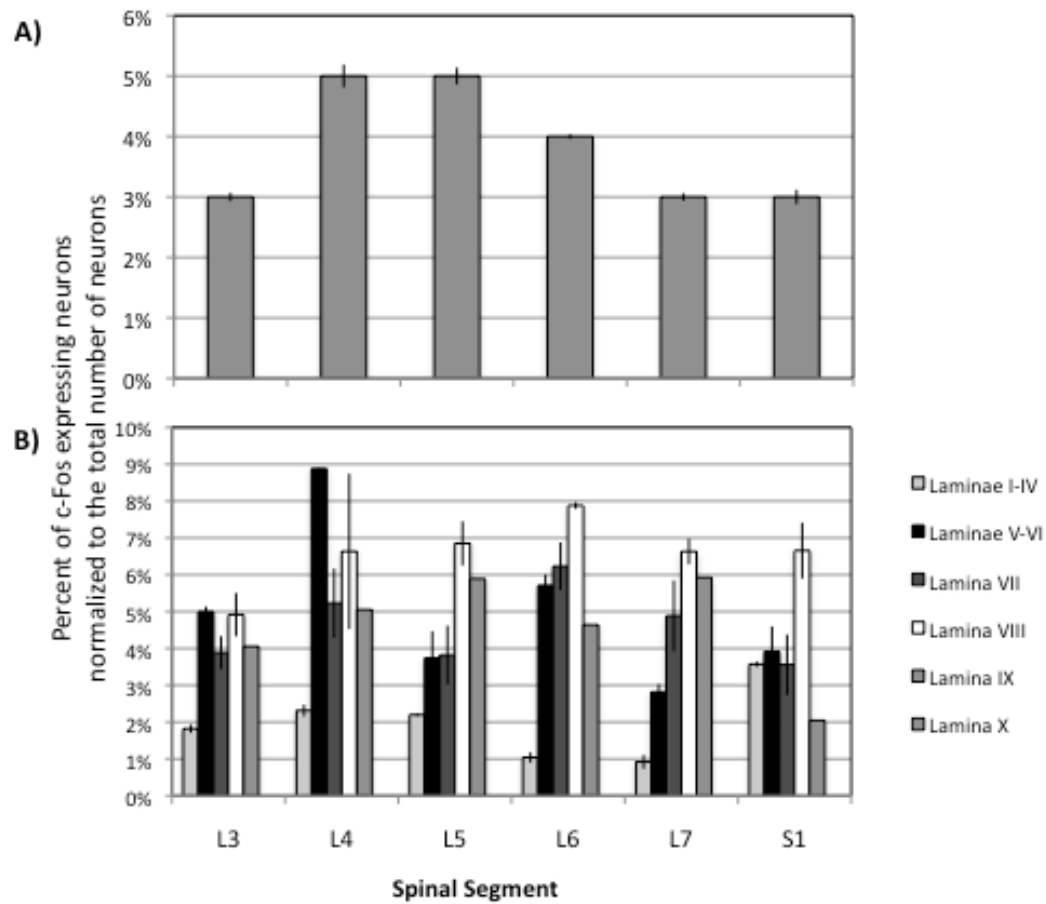


Figure 11. Naïve Control. Low basal levels of c-Fos expression present in the naïve control. Shown is the mean \pm standard error of the percentage of c-Fos positive neurons normalized to the total number of neurons. **A)** Segmental distribution. **B)** Laminar distribution per spinal segment.

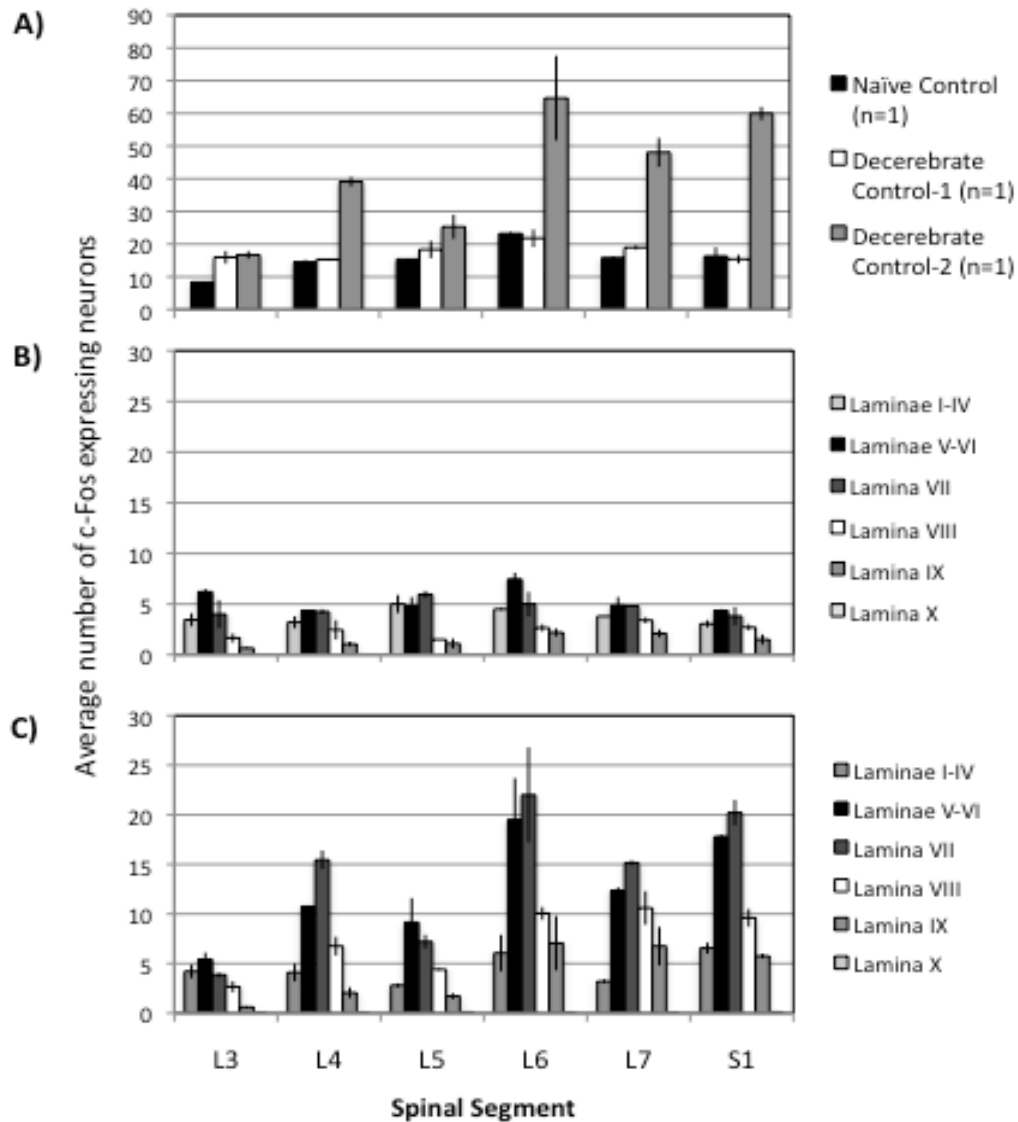


Figure 12. Decerebrate Controls. Shown is the mean \pm standard error of neurons expressing c-Fos, demonstrating the effect of decerebration on c-Fos activation. For each animal, the mean was calculated by averaging the number of c-Fos positive neurons on the left and right sides of the spinal cord for 10 tissue sections, followed by averaging the means of the two hemisections for each spinal segment. **A)** Shows variability between decerebrate control animals in comparison to the naïve control. **B)** Laminar distribution for decerebrate control-1. **C)** Laminar distribution for decerebrate control-2.

3.2.2 Laminectomy

A laminectomy involves removal of the spinous processes of vertebrae enclosing the spinal cord. The surgical preparation is necessary to access the spinal cord for ISMS array implantation. Although a laminectomy does not directly damage the spinal cord, it may have acute effects (Anderson et al., 1978). In the present study, decerebrate-with-laminectomy controls (n=2) were performed to determine the effect of an acute laminectomy on c-Fos expression in the spinal cord [Figure 13]. One of the decerebrate-with-laminectomy controls demonstrated a remarkable increase in c-Fos across all spinal segments compared to the naive and decerebrate control animals. The majority of c-Fos expression was located in laminae V-VIII. However, c-Fos expression levels for the second decerebrate-with-laminectomy control were not as high and more similarly resembled activation levels for the decerebrate controls. The results reveal variability between animals, but demonstrate that a laminectomy can have a substantial influence on the extent of c-Fos activation.

3.3 Effects of Acute ISMS Array Implantation

It has previously been shown that chronic ISMS array implants produce an on-going immune response that results in the formation of glial scarring around the microwires (Bamford et al., 2010). However, the acute response of microwire implantation has not yet been investigated; therefore, the present study performed sham ISMS controls (n=3), which received ISMS array implantation and no electrical stimulation, to determine the effect of microwire implantation on c-Fos

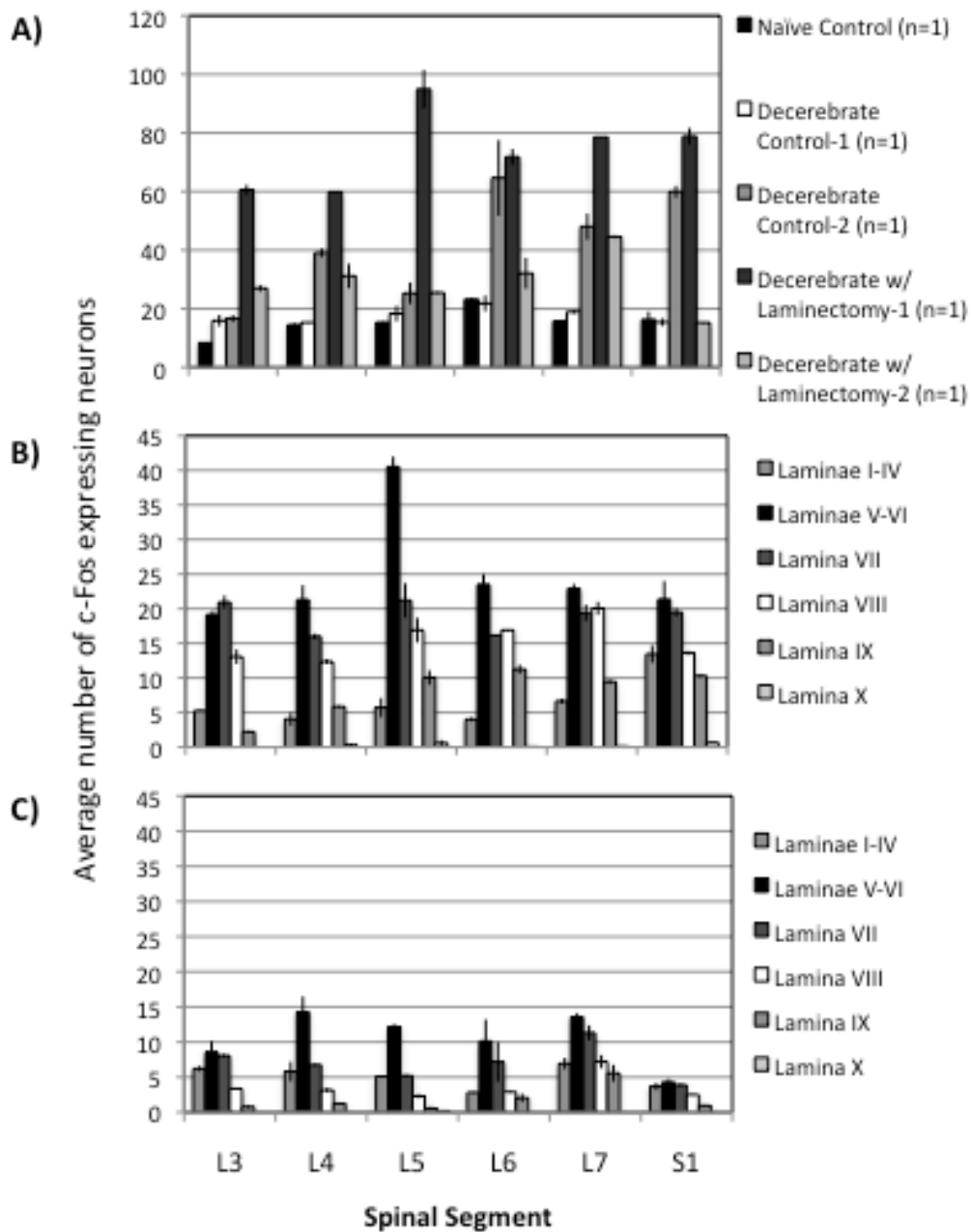


Figure 13. Decerebrate-with-Laminectomy Controls. Shown is the mean \pm standard error of neurons expressing c-Fos, demonstrating the effect of a laminectomy on c-Fos activation. For each animal, the mean was calculated by averaging the number of c-Fos positive neurons on the left and right sides of the spinal cord for 10 tissue sections, followed by averaging the means of the two hemisections for each spinal segment. **A)** The increase in c-Fos expression for decerebrate-with-laminectomy control animals is variable compared to naïve and decerebrate controls. **B)** Laminar distribution for decerebrate-with-laminectomy control-1. **C)** Laminar distribution for decerebrate-with-laminectomy control-2.

expression. During serial sectioning of the spinal cord, microwire tracks were located in only a few tissue sections. These revealed an accumulation of c-Fos positive neurons and presumably immune cells surrounding the track [Figure 14]. However, the response appeared to be localized immediately around the microwires and did not influence the longitudinal distribution of c-Fos expression, as there were no substantial peaks of c-Fos expression in the spinal segments where an ISMS array was implanted [Figure 15]. Generally, the segmental distribution was similar between the sham ISMS controls even though the array implantation sites were located in different regions of the spinal cord [Figure 15]. The amount of c-Fos expression was variable between the sham ISMS controls; however, all animals showed a substantial increase of c-Fos positive neurons compared to the naive control [Figure 16]. The sham ISMS controls also demonstrated an increase of c-Fos positive neurons compared to decerebrate and decerebrate-with-laminectomy control animals [Figure 17].

3.4 Effects of ISMS stimulation

3.4.1 ISMS without Surveillance

Animals receiving ISMS without stimulation surveillance were given injections of a NMJ blocker to remove the influence of proprioceptive feedback on c-Fos activation in the spinal cord. The effect of stimulation could not be monitored due to the paralyzing effects of the drug. Surprisingly, data from the experimental group revealed similar c-Fos expression levels in the left and right hemispheres even though electrical stimulation was only applied to one side of the

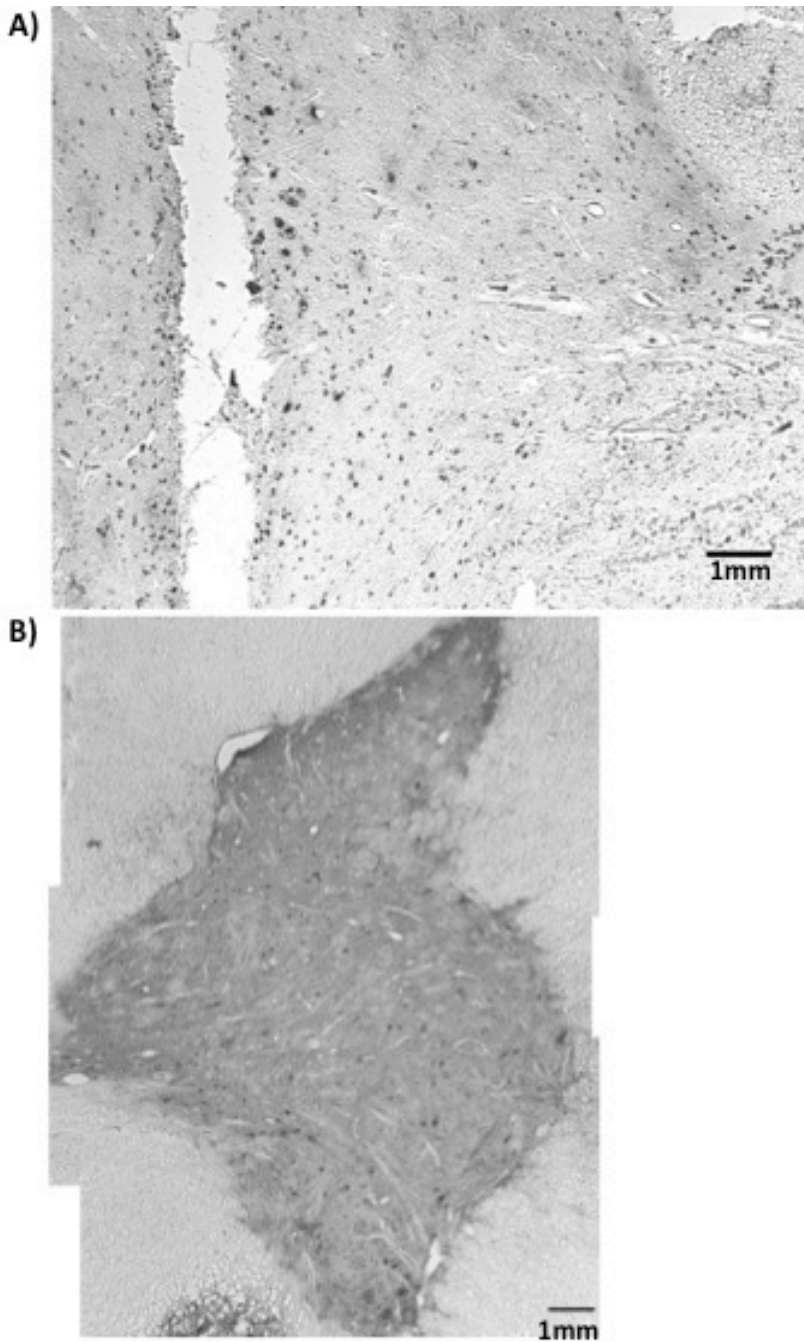


Figure 14. Images of the Effect of Microwire Insertion. A) Accumulation of c-Fos expressing cells around the microwire track. B) Cross-section from a spinal segment with implanted microwires, which demonstrates dispersed c-Fos expression and suggests it was not affected by the microwires.

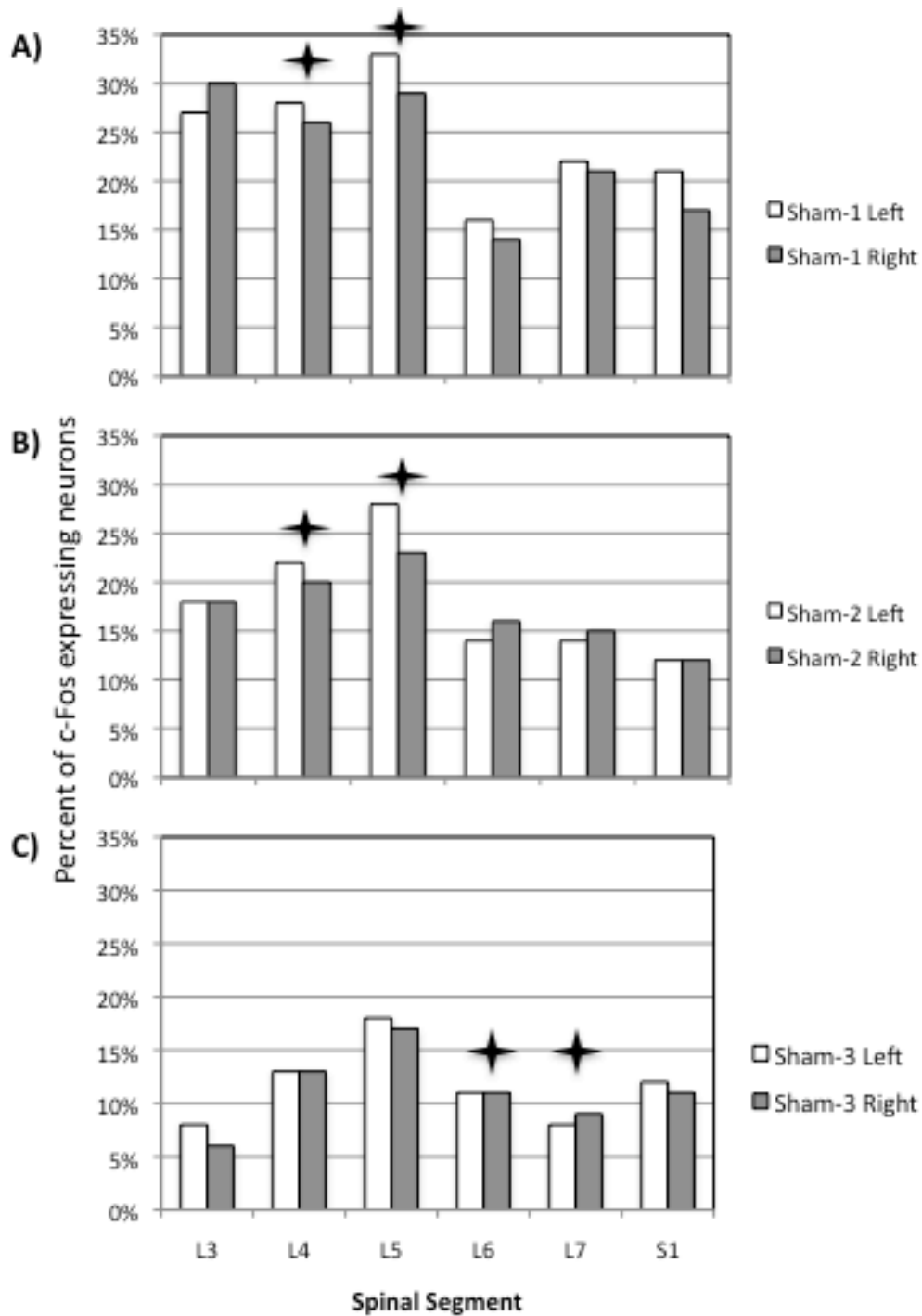


Figure 15. Effect of Microwire Insertion. Shown is the segmental distribution of c-Fos expressing neurons normalized to the total number of neurons. Stars represent the location of array implantation. The sham controls generally had the same distribution across spinal segments and did not show substantial peaks in c-Fos within the region where the microwire arrays were implanted. **A)** Sham ISMS control-1. **B)** Sham ISMS control-2. **C)** Sham ISMS control-3.

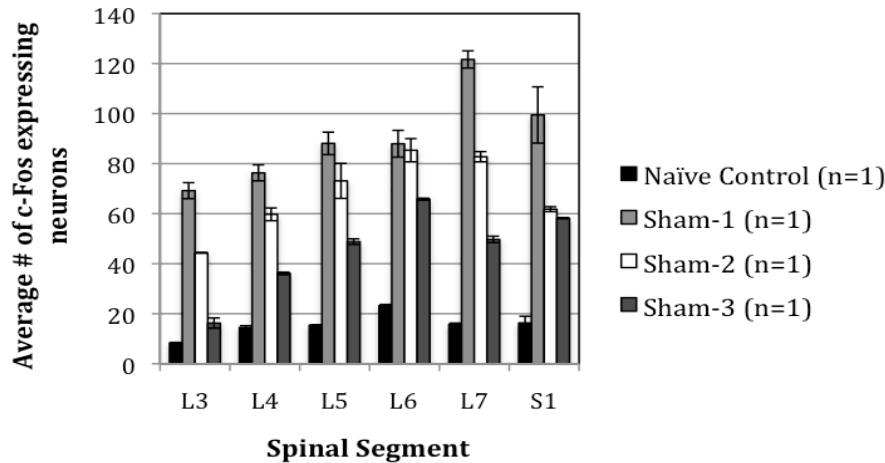


Figure 16. Sham ISMS Controls. The amount of c-Fos expression varies among sham ISMS animals. Shown is the mean \pm standard error of neurons expressing c-Fos. The mean was calculated by averaging the number of c-Fos positive neurons on the left and right sides of the spinal cord for 10 tissue sections, followed by averaging the means of the two hemisections for each spinal segment. All sham ISMS controls demonstrated a substantial increase of c-Fos-positive neurons compared to the naïve control.

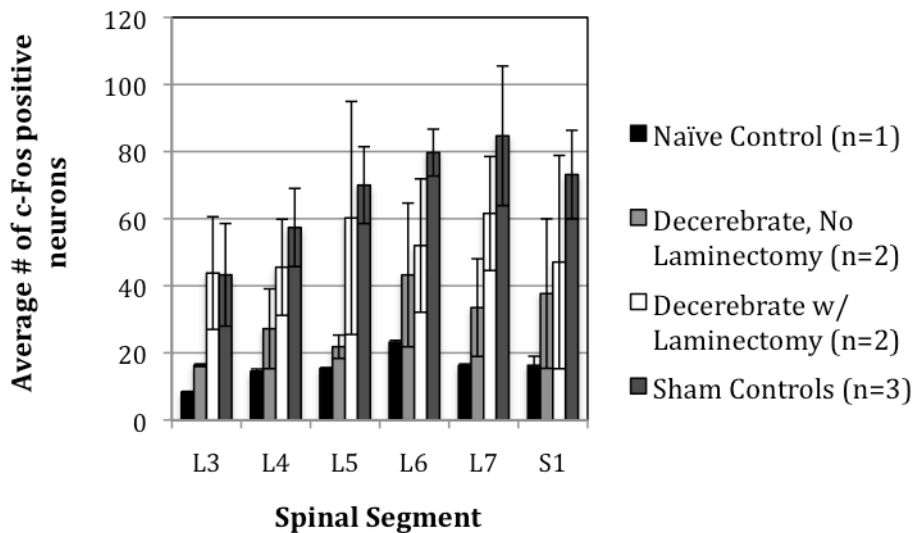


Figure 17. Comparison of Control Groups. Shown is the mean \pm standard error of neurons expressing c-Fos for the following experimental conditions: naïve control, decerebrate controls, decerebrate-with-laminectomy controls, and sham ISMS controls. The mean was calculated by averaging the number of c-Fos positive neurons on the left and right sides of the spinal cord for 10 tissue sections, followed by averaging the means of the two hemisections for each spinal segment, then averaging across animals within the same experimental group. Sham ISMS control animals exhibited the highest counts of c-Fos through L4-S1 spinal segments.

spinal cord [Figure 18]. According to the laminar distribution, the highest levels of c-Fos expression were present in laminae V-VII. Positive control animals showed a substantial increase in c-Fos expression on the stimulated side relative to the contralateral non-stimulated side. Therefore, the results raised concerns regarding sustained effectiveness of ISMS throughout the duration of stimulation and further experiments were performed to monitor the effectiveness of ISMS during the 3-hour stimulation time period.

3.4.2 ISMS with Surveillance

The effectiveness of the stimulation protocol utilized for the present study was monitored in non-decerebrate animal preparations (n=2). The NMJ blocker was not administered; therefore, the extensor synergy could be monitored visually and the stimulation amplitude adjusted accordingly to maintain a consistent force production throughout the 3-hour stimulation time frame. The required adjustments in stimulus amplitude differed between the two animals. One cat required an increase of 70 μ A (100 μ A- 170 μ A) or a 70% increase in stimulation amplitude over the first 2 ½ hours of stimulation. The second cat only needed a 40 μ A (100 μ A- 140 μ A) or 40% increase in stimulation amplitude during the first 25 minutes.

A complete segmental distribution of c-Fos could not be obtained for these animals due to damage to the rostral segments of the spinal cord during the laminectomy. Although surgical procedures were performed carefully, even slight perturbations to the spinal cord could impair the blood-spinal cord barrier,

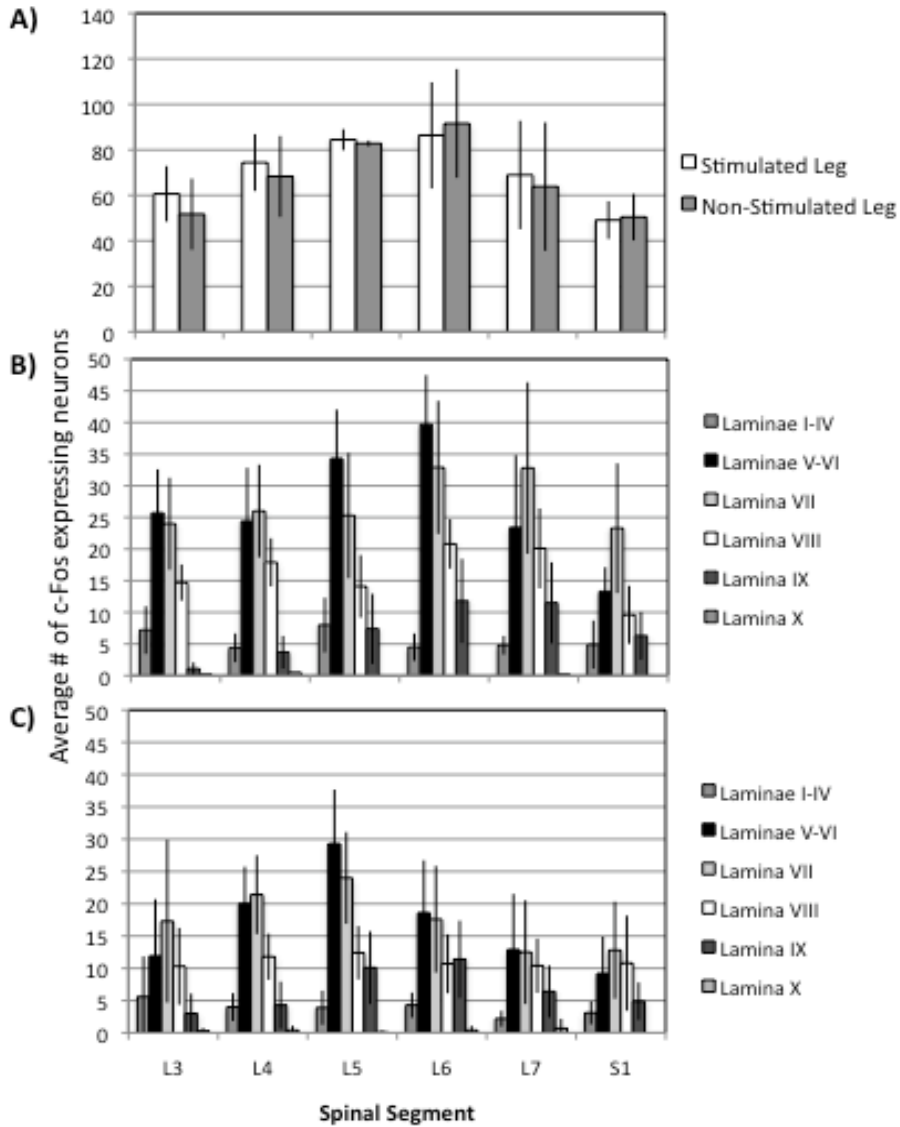


Figure 18. Extensor ISMS without Surveillance. **A)** Shown is the mean \pm standard error for the segmental distribution of c-Fos expression for ISMS animals (n=2) stimulated without surveillance. For each animal, the average number of c-Fos positive neurons on the stimulated and non-stimulated sides of the spinal cord was calculated for 10 tissue sections. The mean represented in the graph was calculated by averaging the means from the two hemisections for each spinal segment across the two animals in the experimental group. Results revealed an equivalent number of c-Fos expressing neurons for the stimulated and non-stimulated sides of the spinal cord. **B)** Laminar distribution of the stimulated side for extensor ISMS-1 without surveillance (mean \pm standard deviation of ten slices per spinal segment). **C)** Laminar distribution of the stimulated side for extensor ISMS-2 without surveillance (mean \pm standard deviation of ten slices per spinal segment).

resulting in hemorrhaging. The presence of blood in the spinal cord resulted in an intense increase of c-Fos expression in neurons and presumably in infiltrating immune cells [Figure 19]. The effect confounded the ability to determine the distribution of ISMS-activated neurons.

Nonetheless, c-Fos expression could be analyzed for the L6 and L7 spinal segments, which was the region of microwire array implantation and stimulation. Data showed an increase of c-Fos expression in the stimulated hemisphere compared to the non-stimulated side of the spinal cord for both spinal segments; however, the difference in activation levels between hemispheres was not as pronounced in L7 relative to L6 [Figure 20]. These results suggest that ISMS can induce an additive amount of c-Fos activation beyond experimental conditions.

Due to differences in surgical preparations, data from ISMS animals with stimulation surveillance cannot be compared to other experimental groups. These non-decerebrate animals were stimulated under the administration of sodium pentobarbital, while all other groups were stimulated following decerebration and the removal of anesthetic. It is well known that anesthesia suppresses c-Fos activation; therefore, reducing the amount of c-Fos visualization with IHC (Jinks et al., 2002).

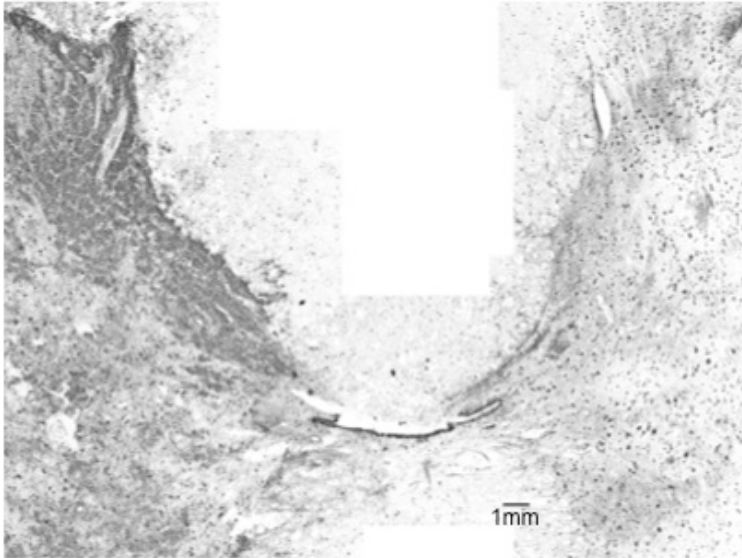


Figure 19. Effect of Hemorrhaging in the Spinal Cord. Spinal cord cross-section demonstrates the damaging effect of hemorrhaging and the influence on c-Fos expression. The left side of the spinal cord shows hemorrhagic tissue, while the right side displays immense c-Fos immunostaining.

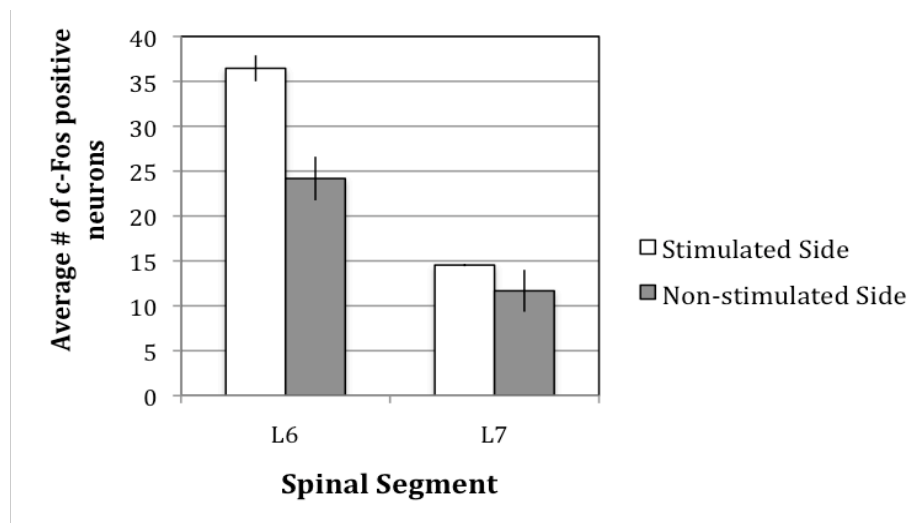


Figure 20. Extensor ISMS with surveillance. C-Fos expression in L6 and L7 spinal segments for extensor ISMS cats with stimulation surveillance (n=2). Shown is the mean \pm standard error of neurons expressing c-Fos. For each animal, the average number of c-Fos positive neurons on the stimulated and non-stimulated sides of the spinal cord was calculated for 10 tissue sections. The mean represented in the graph was calculated by averaging the means from the two hemisections for each spinal segment across the two animals in the experimental group. C-Fos expression was increased in the stimulated side relative to the non-stimulated side of the spinal cord.

3.5 Summary of Results

The present study was successful in optimizing an IHC protocol for c-Fos, which demonstrated the benefits of utilizing antigen retrieval techniques. Heating tissue in citrate buffer prior to immunostaining improved visualization by increasing the number of c-Fos positive neurons, including motoneurons. Although results were variable, both decerebration and laminectomy surgical procedures influenced the activation of c-Fos in the spinal cord; however, effects from the laminectomy were more substantial. C-Fos expression for un-monitored ISMS-stimulated animals was similar for the left and right hemispheres. ISMS-stimulated animals with surveillance received periodical increases in stimulus amplitude and demonstrated an elevated amount of c-Fos in the stimulated side versus the non-stimulated side of the spinal cord.

4. Discussion

The goal of the present study was to develop appropriate experimental methodology to investigate the mechanisms of action of ISMS. A c-Fos IHC protocol was optimized to map distributions of activated neurons, including motoneurons. The study investigated the influence of the experimental setup on inducing c-Fos expression in the cat spinal cord, which confounded the ability to determine the neuronal networks activated by ISMS. The data aided in the development of a protocol to achieve the original aim of the study in understanding the mechanisms of action of ISMS.

4.1 Antigen Retrieval Techniques

Protocols for IHC have not always utilized antigen retrieval techniques. The use of heat-induced antigen retrieval has become popular, as it has been shown to enhance antigenicity (Shi et al., 1991). Fixation of tissue reduces immunoreactivity because formaldehyde reduces antigenicity by reacting with the epitope, causing formation of protein cross-links that masks the antigen, or changing protein configurations (O'Leary et al., 2009). The successes of heat-induced retrieval techniques are attributed to reversing the effects of fixation (O'Leary et al., 2009). Antigen retrieval methods may not be vital when qualitatively comparing regions of activity. However, the present study demonstrated the necessity of retrieval techniques to obtain accurate

quantifications and mapping of c-Fos-positive neurons.

The lack of c-Fos visualization in motoneurons has previously been discussed and attributed to neuronal habituation from repetitive activation following electrical stimulation (Dai et al., 2005) or reduced expression levels that are too low for IHC detection (Hunt et al., 1987). Another study showed that motoneurons can express c-Fos, but expression is delayed by approximately 8 hours, following stimulation (Dampney et al., 1995). However, observations from the present study revealed that the determining factor for the visualization of c-Fos expression in motoneurons may be the use of heat-induced antigen retrieval methods.

Data from IHC optimization trials showed that the positive control animal had substantially more c-Fos expression than ISMS or sham ISMS animals. It was expected that the sham ISMS control would have less neuronal activation, as the animal's spinal cord was not electrically stimulated. Unexpectedly, the ISMS animal (without stimulation surveillance) had similar numbers of c-Fos expression compared to the sham ISMS; however, the effectiveness of ISMS in producing a consistent extensor synergy throughout the duration of stimulation was unknown, as it was unable to be monitored. It would be expected that dorsal root stimulation would express more c-Fos than ISMS with stimulation surveillance, as it non-selectively activates mixed afferent fibers (i.e. group I & II sensory afferents), while ISMS activates a specific network of neurons.

4.2 Experimental Conditions

Concerns regarding the experimental protocol arose after reviewing results from sham ISMS control and ISMS without surveillance animals, as the two groups revealed similar levels of c-Fos expression. Additionally, c-Fos expression levels were similar in the left and right hemispheres for ISMS without surveillance animals, even though stimulation was only applied to one side of the spinal cord. Although some neurons project contralaterally to activate neurons on the non-stimulated side, it was expected that c-Fos expression would be more substantial in the stimulated side of the spinal cord. This was anticipated because results from dorsal root stimulation showed elevated levels of c-Fos expression on the stimulated hemisphere (151 c-Fos expressing neurons) versus the non-stimulated hemisphere (105 c-Fos expressing neurons) of the spinal cord. These concerns led to the completion of additional experimental control groups to understand if factors in the protocol were confounding the ability to map the distribution of ISMS-activated neurons. As expected, the naive control animal showed low basal c-Fos expression; however, the surgical preparations utilized for the remaining control groups increased the background c-Fos levels.

4.2.1 Decerebration

Following decerebration, inhibition to the spinal cord is removed, generating a descending excitatory drive that results in recurring prolonged spasms (Sherrington, 1898). The magnitude of excitation varies according to the location and angle of decerebration (Grillner and Shik, 1973). A rostral, pre-

mammillary decerebration results in spontaneous locomotion on a treadmill, while the generation of locomotor-like activity following a post-mammillary, pre-collicular decerebration requires stimulation near the cuneiforme nucleus. Inducible locomotion is terminated with a further caudal, inter-collicular trans-section, which was utilized in the present study (Grillner and Shik, 1973). Variability of cerebral trans-section angles and levels of excitability between animals is inevitable. Therefore, the study determined the impact of an inter-collicular decerebration on c-Fos activation in the spinal cord.

Results from decerebrate control animals demonstrated that decerebrate excitability has less of an impact on spinal c-Fos expression than other surgical procedures. However, variability in the number of c-Fos positive neurons was present, which may be attributable to different amounts of spinal excitability from inconsistencies in the decerebration procedure. The disadvantage to the experimental preparation was that the amount or presence of spinal excitability for the animals was unknown, as a NMJ blocker was administered 1-hour post-decerebration. Previous studies have also utilized the decerebrate cat preparation to investigate c-Fos activation in the spinal cord following central and peripheral stimulation. Comparably, sham controls revealed low levels of c-Fos expression, similar to a naive control (Dai et al., 2005; Gustafson et al., 2006). Based on results from the present and previous studies, it is concluded that the decerebrate cat preparation is acceptable for future c-Fos immunostaining studies in the spinal cord.

4.2.2 Laminectomy

The amount of c-Fos expression was also variable between decerebrate-with-laminectomy controls. The invasive laminectomy procedure affected each animal differently, causing varying amounts of blood loss. A study performed by Anderson et al. [1978] revealed that spinal cord blood flow following a laminectomy was reduced by 22-45%, possibly as a result of vasoconstriction. Blood flow levels returned to baseline 24 hours post-laminectomy (Anderson et al., 1978). Additionally, it has been shown that ischemia produced by occlusion of the cerebral artery induces c-Fos expression in the rat spinal cord (Wu et al., 1997). The mechanism is unknown; however, it may be linked to glutamate release or influx of calcium following ischemia (Wu et al., 1997). Therefore, it is plausible to suggest that diminished blood flow to the spinal cord could cause neuronal stress, resulting in activation of the c-Fos pathway. Results from the decerebrate-with-laminectomy controls revealed increased numbers of c-Fos-positive neurons compared to naïve and decerebrate control animals. In conclusion, it is suggested that assessment of ISMS-activated neurons be performed long after (e.g., 1 week or more) the laminectomy procedure to allow for the return of normal blood flow levels. This can be done by conducting the experiments in animals with chronically implanted ISMS arrays.

4.2.3 Microwire Implantation

Variability of c-Fos expression between sham control animals, which received ISMS array implantation, but no stimulation, may be explained by the

effects of decerebration and laminectomy. Interestingly, the acute procedure of implanting microwires into the spinal cord resulted in a localized increase of c-Fos expression that did not influence the c-Fos distribution along the lumbosacral enlargement. Although the effect of implantation was not substantial, it would be beneficial to perform ISMS array implantation chronically with the laminectomy. Therefore, all surgical procedures on the spinal cord would be performed prior to the day of the stimulation protocol, allowing for recovery.

4.2.4 ISMS

Data from extensor ISMS animals with surveillance demonstrated the ability of ISMS to generate a full-limb extensor synergy across the hip, knee, and ankle joints for the duration of the stimulus protocol. However, the animals required different adjustments in stimulus amplitude to maintain a consistent, forceful synergy. Rationale behind the observation can be explained in two ways. One consideration is the location of the microwire tips within the grey matter, as differences in stimulation sites result in varying synergistic responses. Placement of the microwires in the motoneuron pools is based on functional output following application of electrical stimulation; however, due to the absence of visibility during implantation, it is difficult to target identical locations in the lumbosacral enlargement of the spinal cord for each animal. The second consideration for differences in required stimulus amplitude is the physiological condition of each animal, as reduced force production is a result of fatiguing motor units. The first cat, which required fewer increases in stimulus amplitude, was extremely active. Therefore, his muscles likely contained a high proportion of slow fatigue-resistant

fibers. A more substantial increase in stimulation amplitude was necessary for the second cat, which was overweight and therefore, his muscles may have been mainly composed of fast fatigable fibers. Both explanations demonstrate the importance of monitoring the stimulation, as output varies between animals. Additionally, as shown for the ISMS animals with stimulation surveillance and positive controls, maintaining a consistent, forceful extensor synergy allows for an increase in c-Fos expression on the stimulated side of the spinal cord to be observed beyond the background levels of surgically induced c-Fos.

4.3 Mapping Studies

4.3.1 Central Pattern Generator

The CPG, which is the network of neurons in the spinal cord that generates rhythmic locomotion, is difficult to study in a normal functioning animal preparation (Kiehn, 2006). Current methods utilized to activate the spinal cord include the application of pharmacological agents and electrical stimulation of the peripheral nerves or descending tracts (Cazalets et al., 1995; Dai et al., 2005; Gustafson et al., 2006). Utilizing dorsal root stimulation and electromyographic recordings following serial lesioning of the spinal cord, Grillner and Zangger demonstrated the rostro-caudal extent of the CPG in the lumbar enlargement of the spinal cord (Grillner and Zangger, 1979). However, the organization of the CPG remains a topic of debate (Kiehn, 2006).

4.3.2 c-Fos Mapping Studies

Investigators have utilized both direct (cellular recordings) and indirect (immunohistochemistry) techniques to identify regions of neuronal activity in the lumbosacral enlargement that may contribute to the function of the CPG (Kiehn and Kjaerulff, 1998). IHC of the activity-dependent marker c-Fos is a functional mapping technique widely utilized for many cell types, including the spinal cord, endothelial cells, lymphocytes, brain, and brainstem (Lampugnani et al., 1990; Ogawa et al., 1997; Ahn et al., 2008; Jakus et al., 2008; Maeda et al., 2009). More specifically, c-Fos IHC has been utilized to locate activated neuronal networks in the cat spinal cord following various forms of stimuli. Gustafson mapped neurons involved in the hindlimb flexor reflex following peripheral nerve stimulation and reported the majority of c-Fos expression to be localized in laminae I, II, and IV-VII, peaking within spinal segments L6 and L7 (Gustafson et al., 2006). Dai described the neuronal distributions involved during treadmill locomotion induced by stimulation of the mesencephalic locomotor region. Dai reported the most pronounced levels of c-Fos expression in laminae VII-VIII for all lumbosacral spinal segments, but peaking in segment L6 (Dai et al., 2005). C-Fos mapping between the two studies differed, as Gustafson stimulated the spinal cord via sensory afferents, resulting in dorsal horn neuronal activation, while Dai revealed interneurons activated by descending networks from the midbrain. Unlike Gustafson, Dai demonstrated activation of commissural interneurons in lamina VIII, which are responsible for controlling alternations between the hindlimbs.

4.3.3 Understanding the mechanisms of action of ISMS

Without the need to apply pharmacological agents or perform spinal transections, the ISMS technique can stimulate the spinal cord *in vivo*, which may be conducive to understanding the overall organization of the CPG neuronal networks in the spinal cord that are involved in controlling locomotion. The present study optimized a c-Fos IHC protocol that can provide a map of activated neurons to contribute information on the mechanisms of action of ISMS. Electroneurography of spinal dorsal roots and electromyography of hindlimb muscles have been utilized to record cellular activity and determine the extent of ISMS activation (Gaunt et al., 2006; Calixto, 2007). Results showed that ISMS activates neurons in the immediate vicinity of a microwire, as well as up to 17 mm rostrally and caudally. Gaunt's study suggested that ISMS activates motoneurons directly and sensory afferents antidromically, which transsynaptically further activate interneurons and motoneurons (Gaunt et al., 2006). Single unit extracellular recordings in a deafferented cat preparation revealed that ISMS additionally activates propriospinal projections (Calixto, 2007). Therefore, electrical current from ISMS travels through fibers-in-passage, which include interneurons, propriospinal interneuronal connections, and sensory afferents to activate an extensive rostro-caudal distribution of neurons (Gaunt et al., 2006; Calixto, 2007).

4.4 Limitations

There were several limitations within the present study. Due to the large number of experimental groups performed, the minimal sample size was selected to reduce the number of cats. A general trend among experimental groups could be observed and utilized to develop future experimental methodology. However, variability was present between animals in the same experimental groups, which could have been clarified with a larger sample size. Another limitation was the lack of normalization of c-Fos expression to the total number of neurons for each cat, as the number of neurons can vary between animals. For ISMS-stimulated animals, there was variability between synergistic motor responses due to the difficulty of placing microwires in an identical location for each animal.

4.4.1 Limitations of c-Fos Immunohistochemistry

C-Fos IHC is a widely utilized tool to identify activated neurons because of the ease of activation of the c-Fos pathway and the simplicity of IHC detection methods. The method is capable of producing anatomical maps of activated neuronal networks as c-Fos is expressed following trans-synaptic activation (Sagar et al., 1988). C-Fos IHC can also be combined with other identification techniques, such as retrograde tracers or double staining with markers for neurotransmitter proteins, which provides information on the function of c-Fos positive neurons (Jankowska and Skoog, 1986; Huang et al., 2000).

Although it is beneficial for c-Fos to be easily induced, investigators must be cautious with experimental methodologies, as additional stress to the animal,

such as handling, surgical preparations, or exposure to a new environment, can also induce c-Fos expression (Cullinan et al., 1995; Krukoff and Khalili, 1997; Montero, 1997). Additionally, it has been extensively demonstrated that general anesthetics have suppressing effects that alter c-Fos expression (Hagihira et al., 1997; Jinks et al., 2002). ISMS activates both excitatory and inhibitory neurons located in the lumbosacral enlargement of the spinal cord that collaboratively produce rhythmic locomotion (Calixto, 2007). However, a major limitation of c-Fos IHC is that neurons with net inhibitory input do not express c-Fos (Kovacs, 1998). Furthermore, antidromically-activated neurons do not express c-Fos, as trans-synaptic activation is required (Luckman et al., 1994). Therefore, false-negatives can occur when utilizing c-Fos IHC. Although c-Fos immunostaining is useful for labeling activated neurons, these limitations should be kept in consideration when utilizing this technique.

4.5 Suggestions for Future Experiments

Based on findings from the present study, the following recommendations can be made to achieve accurate mapping of ISMS-activated neurons. A decerebrate animal preparation with a chronic spinal cord injury and chronic array implantation would be necessary to minimize surgically-induced background levels of c-Fos expression. 1) A chronic SCI at spinal segment T10 would remove c-Fos activation following decerebrate excitation. 2) A laminectomy and ISMS array implantation performed approximately 1 month prior to the acute experiment would allow the animal to fully recover. Surgically-induced c-Fos

would be reduced as all surgical preparations on the spinal cord would be completed prior to the delivery of the stimulus protocol. 3) A decerebration would be required to remove anesthesia and obtain full c-Fos visualization. 4) Lastly, data from the ISMS with stimulation surveillance animals revealed that monitoring stimulation and adjusting stimulus amplitude are required to maintain a consistent, forceful extensor synergy. The effect of stimulation can be monitored with or without the administration of a NMJ blocker. In the absence of the NMJ blocker, the output can be monitored visually; however, the influence of proprioceptive feedback from the moving hindlimb on c-Fos expression would have to be taken into consideration. The suggested method to monitor the effect of ISMS is to administer a NMJ blocker and monitor the stimulation using electroneurography recordings.

IHC of the activity-dependent marker c-Fos is a feasible technique with the proper methodology in place. If issues utilizing c-Fos still persist, the use of other neuronal markers (i.e. 2-deoxyglucose, sulforhodamine, or calcium imaging) may be investigated; however, these labeling methods also have disadvantages, such as cost, reduced cellular resolution, and ease of employment.

With appropriate experimental methodology, it is hypothesized that immunostaining of ISMS-activated neurons will reveal different staining patterns of neurons that are involved in the production of flexor and extensor synergies. It is expected that an ISMS-induced flexor synergy will produce a staining pattern shifted more rostrally in the lumbosacral enlargement than the distribution obtained following an extensor synergy, as hip flexor muscles are located more

rostrally than hip extensors (Yakovenko et al., 2002). The rostro-caudal extent of ISMS-activated neurons will further demonstrate that ISMS is capable of activating neurons located several millimeters away. Based on the laminar localization of activated neurons, the neurons can be functionally classified (Rexed, 1954).

4.6 Conclusions

The present study investigated the effects of surgical preparations on c-Fos expression in the cat spinal cord, as well as the effectiveness of ISMS in producing synergistic hindlimb movements. These data may be used in developing the appropriate experimental methodology necessary for mapping distributions of ISMS-activated neuronal networks.

Bibliography

Aguayo, AJ, S David, and GM Bray. 1981. Influences of the glial environment on the elongation of axons after injury: transplantation studies in adult rodents. *J Exp Biol* 95, 231-240.

Ahn, SN, JJ Guu, AJ Tobin, VR Edgerton, and NJ Tillakaratne. 2008. Use of c-fos to identify activity-dependent spinal neurons after stepping in intact adult rats. *Cough* 4, 547-559.

Amador, MJ, and JD Guest. 2005. An appraisal of ongoing experimental procedures in human spinal cord injury. *J Neurol Phys Ther* 29, no. 2: 70-86.

Anderson, DK, GR Nicolosi, ED Means, and LE Hartley. 1978. Effects of laminectomy on spinal cord blood flow. *J Neurosurg* 48, no. 2: 232-238.

Anderson, KD. 2004. Targeting recovery: priorities of the spinal cord-injured population. *J Neurotrauma* 21, no. 10: 1371-1383.

Bamford, JA, CT Putman, and VK Mushahwar. 2005. Intraspinal microstimulation preferentially recruits fatigue-resistant muscle fibres and generates gradual force in rat. *J Physiol* 569, no. Pt 3: 873-884.

Bamford, JA, KG Todd, and VK Mushahwar. 2010. The effects of intraspinal microstimulation on spinal cord tissue in the rat. *Biomaterials* 31, no. 21: 5552-5563.

Beattie, MS, AA Farooqui, and JC Bresnahan. 2000. Review of current evidence for apoptosis after spinal cord injury. *J Neurotrauma* 17, no. 10: 915-925.

Berkowitz, A. 2001. Rhythmicity of spinal neurons activated during each form of fictive scratching in spinal turtles. *J Neurophysiol* 86, no. 2: 1026-1036.

Blight, AR. 2002. Miracles and molecules--progress in spinal cord repair. *Nat Neurosci* 5 Suppl, 1051-1054.

Blight, AR, and W Young. 1989. Central axons in injured cat spinal cord recover electrophysiological function following remyelination by Schwann cells. *J Neurol Sci* 91, no. 1-2: 15-34.

Boulenguez, P, and L Vinay. 2009. Strategies to restore motor functions after spinal cord injury. *Curr Opin Neurobiol* 19, no. 6: 587-600.

Brissot, R, P Gallien, MP Le Bot, A Beaubras, D Laisne, J Beillot, and J Dassonville. 2000. Clinical experience with functional electrical stimulation-assisted gait with Parastep in spinal cord-injured patients. *Spine (Phila Pa 1976)* 25, no. 4: 501-508.

Brown, GT. 1911. The Intrinsic Factors in the Act of Progression in the Mammal. *Proceedings of the Royal Society of London. Series B, Containing Papers of a Biological Character* 84, 308-319.

Bunge, RP, WR Puckett, JL Becerra, A Marcillo, and RM Quencer. 1993. Observations on the pathology of human spinal cord injury. A review and classification of 22 new cases with details from a case of chronic cord compression with extensive focal demyelination. *Adv Neurol* 59, 75-89.

Calixto. 2007. Single Cell Recordings During Intraspinial Microstimulation of the Feline Spinal Cord. *Master's Thesis*. University of Alberta.

Carlson, SL, ME Parrish, JE Springer, K Doty, and L Dossett. 1998. Acute inflammatory response in spinal cord following impact injury. *Exp Neurol* 151, no. 1: 77-88.

Cazalets, JR, M Borde, and F Clarac. 1995. Localization and organization of the central pattern generator for hindlimb locomotion in newborn rat. *J Neurosci* 15, no. 7 Pt 1: 4943-4951.

Chida, K, S Nagamori, and T Kuroki. 1999. Nuclear translocation of Fos is stimulated by interaction with Jun through the leucine zipper. *Cell Mol Life Sci* 55, no. 2: 297-302.

Choi, DW. 1987. Ionic dependence of glutamate neurotoxicity. *J Neurosci* 7, no. 2: 369-379.

Chopp, M, XH Zhang, Y Li, L Wang, J Chen, D Lu, M Lu, and M Rosenblum. 2000. Spinal cord injury in rat: treatment with bone marrow stromal cell transplantation. *Neuroreport* 11, no. 13: 3001-3005.

Christopher and Dana Reeve Foundation. 2009. One Degree of Separation: Paralysis and Spinal Cord Injury in the United States.

Colombo, G, M Joerg, R Schreier, and V Dietz. 2000. Treadmill training of paraplegic patients using a robotic orthosis. *J Rehabil Res Dev* 37, no. 6: 693-700.

Cullinan, WE, JP Herman, DF Battaglia, H Akil, and SJ Watson. 1995. Pattern and time course of immediate early gene expression in rat brain following acute stress. *Neuroscience* 64, no. 2: 477-505.

Curran, T. 1992. Fos and Jun: oncogenic transcription factors. *Tohoku J Exp Med* 168, no. 2: 169-174.

Curran, T, AD Miller, L Zokas, and IM Verma. 1984. Viral and cellular fos proteins: a comparative analysis. *Cell* 36, no. 2: 259-268.

Curran, T, and JI Morgan. 1987. Memories of fos. *Bioessays* 7, no. 6: 255-258.

Dai, X, BR Noga, JR Douglas, and LM Jordan. 2005. Localization of spinal neurons activated during locomotion using the c-fos immunohistochemical method. *J Neurophysiol* 93, no. 6: 3442-3452.

Dampney, RA, YW Li, Y Hirooka, P Potts, and JW Polson. 1995. Use of c-fos functional mapping to identify the central baroreceptor reflex pathway: advantages and limitations. *Clin Exp Hypertens* 17, no. 1-2: 197-208.

David, S, and AJ Aguayo. 1985. Axonal regeneration after crush injury of rat central nervous system fibres innervating peripheral nerve grafts. *J Neurocytol* 14, no. 1: 1-12.

Dijkers, M. 1997. Quality of life after spinal cord injury: a meta analysis of the effects of disablement components. *Spinal Cord* 35, no. 12: 829-840.

Ditor, DS, AE Latimer, KA Ginis, KP Arbour, N McCartney, and AL Hicks. 2003. Maintenance of exercise participation in individuals with spinal cord injury: effects on quality of life, stress and pain. *Spinal Cord* 41, no. 8: 446-450.

Dohrmann, GJ, KM Wick, and PC Bucy. 1973. Spinal cord blood flow patterns in experimental traumatic paraplegia. *J Neurosurg* 38, no. 1: 52-58.

Dubreuil, CI, MJ Winton, and L McKerracher. 2003. Rho activation patterns after spinal cord injury and the role of activated Rho in apoptosis in the central nervous system. *J Cell Biol* 162, no. 2: 233-243.

Dumont, RJ, DO Okonkwo, S Verma, RJ Hurlbert, PT Boulos, DB Ellegala, and AS Dumont. 2001. Acute spinal cord injury, part I: pathophysiologic mechanisms. *Clin Neuropharmacol* 24, no. 5: 254-264.

Dusart, I, and ME Schwab. 1994. Secondary cell death and the inflammatory reaction after dorsal hemisection of the rat spinal cord. *Eur J Neurosci* 6, no. 5: 712-724.

Edgerton, VR, SJ Kim, RM Ichiyama, YP Gerasimenko, and RR Roy. 2006. Rehabilitative therapies after spinal cord injury. *J Neurotrauma* 23, no. 3-4: 560-570.

- Eidelberg, E, LH Nguyen, R Polich, JG Walden. 1989. Transsynaptic degeneration of motoneurons caudal to spinal cord lesions. *Brain Res Bull.* 22, no.1: 39-45.
- Elliott, TR, and RG Frank. 1996. Depression following spinal cord injury. *Arch Phys Med Rehabil* 77, no. 8: 816-823.
- Emery, E, P Aldana, MB Bunge, W Puckett, A Srinivasan, RW Keane, J Bethea, and AD Levi. 1998. Apoptosis after traumatic human spinal cord injury. *J Neurosurg* 89, no. 6: 911-920.
- Faden, AI, M Lemke, RP Simon, and LJ Noble. 1988. N-methyl-D-aspartate antagonist MK801 improves outcome following traumatic spinal cord injury in rats: behavioral, anatomic, and neurochemical studies. *J Neurotrauma* 5, no. 1: 33-45.
- Fawcett, JW. 2006. Overcoming inhibition in the damaged spinal cord. *J Neurotrauma* 23, no. 3-4: 371-383.
- Festoff, BW, S Ameenuddin, PM Arnold, A Wong, KS Santacruz, and BA Citron. 2006. Minocycline neuroprotects, reduces microgliosis, and inhibits caspase protease expression early after spinal cord injury. *J Neurochem* 97, no. 5: 1314-1326.
- Field-Fote, EC, SD Lindley, and AL Sherman. 2005. Locomotor training approaches for individuals with spinal cord injury: a preliminary report of walking-related outcomes. *J Neurol Phys Ther* 29, no. 3: 127-137.
- Fink, SL, and BT Cookson. 2005. Apoptosis, pyroptosis, and necrosis: mechanistic description of dead and dying eukaryotic cells. *Infect Immun* 73, no. 4: 1907-1916.
- Fiskum. 2000. Mitochondrial Participation in Ischemic and Traumatic Neural Cell Death. *Journal of Neurotrauma* 17, 843-855.
- Fouad, K, MM Rank, R Vavrek, KC Murray, L Sanelli, and DJ Bennett. 2010. Locomotion after spinal cord injury depends on constitutive activity in serotonin receptors. *J Neurophysiol* 104, no. 6: 2975-2984.
- Fried, LC, and R Goodkin. 1971. Microangiographic observations of the experimentally traumatized spinal cord. *J Neurosurg* 35, no. 6: 709-714.
- Gao, YJ, and RR Ji. 2009. c-Fos and pERK, which is a better marker for neuronal activation and central sensitization after noxious stimulation and tissue injury? *Open Pain J* 2, 11-17.

Gaunt, RA, A Prochazka, VK Mushahwar, L Guevremont, and PH Ellaway. 2006. Intraspinal microstimulation excites multisegmental sensory afferents at lower stimulus levels than local alpha-motoneuron responses. *J Neurophysiol* 96, no. 6: 2995-3005.

Gillilan, LA. 1958. The arterial blood supply of the human spinal cord. *J Comp Neurol* 110, no. 1: 75-103.

Greenberg, ME, and EB Ziff. 1984. Stimulation of 3T3 cells induces transcription of the c-fos proto-oncogene. *Nature* 311, no. 5985: 433-438.

Grillner, S, and ML Shik. 1973. On the descending control of the lumbosacral spinal cord from the "mesencephalic locomotor region". *Acta Physiol Scand* 87, no. 3: 320-333.

Grillner, S, and P Wallen. 1985. Central pattern generators for locomotion, with special reference to vertebrates. *Annu Rev Neurosci* 8, 233-261.

Grillner, S, and P Zangger. 1979. On the central generation of locomotion in the low spinal cat. *Exp Brain Res* 34, no. 2: 241-261.

Guevremont, L. 2007. Physiologically-based Control Strategies and Functional Electrical Stimulation Paradigms for Restoring Standing and Stepping after Spinal Cord Injury. *PhD Dissertation*. University of Alberta.

Gustafson, KJ, MA Moffitt, X Wang, J Sun, S Snyder, and WM Grill. 2006. Topography of spinal neurons active during hindlimb withdrawal reflexes in the decerebrate cat. *Neuroscience* 141, no. 4: 1983-1994.

Hagihira, S, N Taenaka, and I Yoshiya. 1997. Inhalation anesthetics suppress the expression of c-Fos protein evoked by noxious somatic stimulation in the deeper layer of the spinal cord in the rat. *Brain Res* 751, no. 1: 124-130.

Henneman, E and CB Olson. 1965. Relations between Structure and Function in the Design of Skeletal Muscles. *J Neurophysiol* 28, 581-598.

Hoffman, GE, MS Smith, and JG Verbalis. 1993. c-Fos and related immediate early gene products as markers of activity in neuroendocrine systems. *Front Neuroendocrinol* 14, no. 3: 173-213.

Hornby, TG, DH Zemon, and D Campbell. 2005. Robotic-assisted, body-weight-supported treadmill training in individuals following motor incomplete spinal cord injury. *Phys Ther* 85, no. 1: 52-66.

Hortobagyi, T, L Dempsey, D Fraser, D Zheng, G Hamilton, J Lambert, and L Dohm. 2000. Changes in muscle strength, muscle fibre size and myofibrillar gene expression after immobilization and retraining in humans. *J Physiol* 524 Pt 1, 293-304.

Huang, A, BR Noga, PA Carr, B Fedirchuk, and LM Jordan. 2000. Spinal cholinergic neurons activated during locomotion: localization and electrophysiological characterization. *J Neurophysiol* 83, no. 6: 3537-3547.

Hunt, SP, A Pini, and G Evan. 1987. Induction of c-fos-like protein in spinal cord neurons following sensory stimulation. *Nature* 328, no. 6131: 632-634.

Ino, H. 2003. Antigen retrieval by heating en bloc for pre-fixed frozen material. *J Histochem Cytochem* 51, no. 8: 995-1003.

Jakus, J, I Poliacek, E Halasova, P Murin, J Knocikova, Z Tomori, and DC Bolser. 2008. Brainstem circuitry of tracheal-bronchial cough: c-fos study in anesthetized cats. *Respir Physiol Neurobiol* 160, no. 3: 289-300.

Jankowska, E. 1992. Interneuronal relay in spinal pathways from proprioceptors. *Prog Neurobiol* 38, no. 4: 335-378.

Jankowska, E, P Krutki, and K Matsuyama. 2005. Relative contribution of Ia inhibitory interneurons to inhibition of feline contralateral motoneurons evoked via commissural interneurons. *J Physiol* 568, no. Pt 2: 617-628.

Jankowska, E, and WJ Roberts. 1972. An electrophysiological demonstration of the axonal projections of single spinal interneurons in the cat. *J Physiol* 222, no. 3: 597-622.

Jankowska, E, and B Skoog. 1986. Labelling of midlumbar neurones projecting to cat hindlimb motoneurons by transneuronal transport of a horseradish peroxidase conjugate. *Neurosci Lett* 71, no. 2: 163-168.

Ji, RR, H Baba, GJ Brenner, and CJ Woolf. 1999. Nociceptive-specific activation of ERK in spinal neurons contributes to pain hypersensitivity. *Nat Neurosci* 2, no. 12: 1114-1119.

Jinks, SL, JF Antognini, JT Martin, S Jung, E Carstens, and R Atherley. 2002. Isoflurane, but not halothane, depresses c-fos expression in rat spinal cord at concentrations that suppress reflex movement after supramaximal noxious stimulation. *Anesth Analg* 95, no. 6: 1622-8, table of contents.

Jordan, LM. 1998. Initiation of locomotion in mammals. *Ann N Y Acad Sci* 860, 83-93.

Jordan, LM, J Liu, PB Hedlund, T Akay, and KG Pearson. 2008. Descending command systems for the initiation of locomotion in mammals. *Brain Res Rev* 57, no. 1: 183-191.

Kandel, E, J Schwartz, T Jessel. 1991. *Principles of Neural Science*: Third Edition. Appleton & Lange.

Kiehn, O. 2006. Locomotor circuits in the mammalian spinal cord. *Annu Rev Neurosci* 29, 279-306.

Kiehn, O, and O Kjaerulff. 1998. Distribution of central pattern generators for rhythmic motor outputs in the spinal cord of limbed vertebrates. *Ann N Y Acad Sci* 860, 110-129.

Kobetic, R, CS To, JR Schnellenberger, ML Audu, TC Bulea, R Gaudio, G Pinault, S Tashman, and RJ Triolo. 2009. Development of hybrid orthosis for standing, walking, and stair climbing after spinal cord injury. *J Rehabil Res Dev* 46, no. 3: 447-462.

Kobetic, R, RJ Triolo, and EB Marsolais. 1997. Muscle selection and walking performance of multichannel FES systems for ambulation in paraplegia. *IEEE Trans Rehabil Eng* 5, no. 1: 23-29.

Kovacs, KJ. 1998. c-Fos as a transcription factor: a stressful (re)view from a functional map. *Neurochem Int* 33, no. 4: 287-297.

Krukoff, TL. 1998. c-Fos Expression as a Marker of Functional Activity in the Brain: Immunohistochemistry. *Cell Neurobiology Techniques: Neuromethods* 33, 213-230.

Krukoff, TL, and P Khalili. 1997. Stress-induced activation of nitric oxide-producing neurons in the rat brain. *J Comp Neurol* 377, no. 4: 509-519.

Kutzenberger, J, B Domurath, D Sauerwein. 2005. Spastic bladder and spinal cord injury: seventeen years of experience with sacral deafferentation and implantation of an anterior root stimulator. *Artif Organs*. 29(3): 239-241.

Lampugnani, MG, N Polentarutti, M Pedenovi, A Mantovani, E Dejana, and F Colotta. 1990. c-fos and c-myc expression in human endothelial cells as a function of different culture conditions. *Exp Cell Res* 186, no. 2: 381-384.

Lanska, DJ. 2009. Historical perspective: neurological advances from studies of war injuries and illnesses. *Ann Neurol* 66, no. 4: 444-459.

Lau, B, L Guevremont, and VK Mushahwar. 2007. Strategies for generating prolonged functional standing using intramuscular stimulation or intraspinal microstimulation. *IEEE Trans Neural Syst Rehabil Eng* 15, no. 2: 273-285.

Lee, SM, TY Yune, SJ Kim, DW Park, YK Lee, YC Kim, YJ Oh, GJ Markelonis, and TH Oh. 2003. Minocycline reduces cell death and improves functional recovery after traumatic spinal cord injury in the rat. *J Neurotrauma* 20, no. 10: 1017-1027.

Lehmann, M, A Fournier, I Selles-Navarro, P Dergham, A Sebok, N Leclerc, G Tigyi, and L McKerracher. 1999. Inactivation of Rho signaling pathway promotes CNS axon regeneration. *J Neurosci* 19, no. 17: 7537-7547.

Lewen, A, P Matz, and PH Chan. 2000. Free radical pathways in CNS injury. *J Neurotrauma* 17, no. 10: 871-890.

Liverman CT. 2005. Spinal cord injury: progress, promise, and priorities. The National Academies Press.

Loane DJ, Byrnes KR. 2010. Role of Microglia in Neurotrauma. *Neurotherapeutics: The Journal of the American Society for Experimental NeuroTherapeutics* 7, 366-377.

Luckman, SM, RE Dyball, and G Leng. 1994. Induction of c-fos expression in hypothalamic magnocellular neurons requires synaptic activation and not simply increased spike activity. *J Neurosci* 14, no. 8: 4825-4830.

Lundberg, A, K Malmgren, and ED Schomburg. 1987. Reflex pathways from group II muscle afferents. 1. Distribution and linkage of reflex actions to alpha-motoneurons. *Exp Brain Res* 65, no. 2: 271-281.

Maeda, Y, M Ikeuchi, P Wacnik, and KA Sluka. 2009. Increased c-fos immunoreactivity in the spinal cord and brain following spinal cord stimulation is frequency-dependent. *Brain Res* 1259, 40-50.

Matsuyama, K, S Kobayashi, and M Aoki. 2006. Projection patterns of lamina VIII commissural neurons in the lumbar spinal cord of the adult cat: an anterograde neural tracing study. *Neuroscience* 140, no. 1: 203-218.

Mautes, AE, MR Weinzierl, F Donovan, and LJ Noble. 2000. Vascular events after spinal cord injury: contribution to secondary pathogenesis. *Phys Ther* 80, no. 7: 673-687.

- Mendell, LM, and E Henneman. 1971. Terminals of single Ia fibers: location, density, and distribution within a pool of 300 homonymous motoneurons. *J Neurophysiol* 34, no. 1: 171-187.
- Merkler, D, GA Metz, O Raineteau, V Dietz, ME Schwab, and K Fouad. 2001. Locomotor recovery in spinal cord-injured rats treated with an antibody neutralizing the myelin-associated neurite growth inhibitor Nogo-A. *J Neurosci* 21, no. 10: 3665-3673.
- Miller, RG, JD Mitchell, M Lyon, and DH Moore. 2007. Riluzole for amyotrophic lateral sclerosis (ALS)/motor neuron disease (MND). *Cochrane Database Syst Rev* no. 1: CD001447.
- Montero, C. 2003. The antigen-antibody reaction in immunohistochemistry. *J Histochem Cytochem* 51, no. 1: 1-4.
- Montero, VM. 1997. c-fos induction in sensory pathways of rats exploring a novel complex environment: shifts of active thalamic reticular sectors by predominant sensory cues. *Neuroscience* 76, no. 4: 1069-1081.
- Morgan, JI, and T Curran. 1991. Stimulus-transcription coupling in the nervous system: involvement of the inducible proto-oncogenes fos and jun. *Annu Rev Neurosci* 14, 421-451.
- Murray, M, D Kim, Y Liu, C Tobias, A Tessler, and I Fischer. 2002. Transplantation of genetically modified cells contributes to repair and recovery from spinal injury. *Brain Res Brain Res Rev* 40, no. 1-3: 292-300.
- Mushahwar, VK, DF Collins, and A Prochazka. 2000. Spinal cord microstimulation generates functional limb movements in chronically implanted cats. *Exp Neurol* 163, no. 2: 422-429.
- Mushahwar, VK, and KW Horch. 2000. Muscle recruitment through electrical stimulation of the lumbo-sacral spinal cord. *IEEE Trans Rehabil Eng* 8, no. 1: 22-29.
- Mushahwar, VK, PL Jacobs, RA Normann, RJ Triolo, and N Kleitman. 2007. New functional electrical stimulation approaches to standing and walking. *J Neural Eng* 4, no. 3: S181-97.
- Nashold, BS, H Friedman, JF Glenn, JH Grimes, WF Barry, and R Avery. 1971. Electromyoturbation in paraplegia: implantation of a spinal neuroprosthesis. *Proc Veterans Adm Spinal Cord Inj Conf* 18, 161-165.
- Nomura, H, CH Tator, and MS Shoichet. 2006. Bioengineered strategies for spinal cord repair. *J Neurotrauma* 23, no. 3-4: 496-507.

Noreau, L, and P Fougereyrollas. 2000. Long-term consequences of spinal cord injury on social participation: the occurrence of handicap situations. *Disabil Rehabil* 22, no. 4: 170-180.

Norenberg, MD, J Smith, and A Marcillo. 2004. The pathology of human spinal cord injury: defining the problems. *J Neurotrauma* 21, no. 4: 429-440.

O'Leary, TJ, CB Fowler, DL Evers, and JT Mason. 2009. Protein fixation and antigen retrieval: chemical studies. *Biotech Histochem* 84, no. 5: 217-221.

Ogawa, Y, A Nishioka, N Hamada, M Terashima, T Inomata, S Yoshida, H Seguchi, and S Kishimoto. 1997. Immunohistochemical study of c-fos-positive lymphocytes infiltrated into human squamous cell carcinomas of the head and neck during radiation therapy and its clinical significance. *Clin Cancer Res* 3, no. 12 Pt 1: 2301-2307.

Olney, JW, OL Ho, and V Rhee. 1971. Cytotoxic effects of acidic and sulphur containing amino acids on the infant mouse central nervous system. *Exp Brain Res* 14, no. 1: 61-76.

Otali, D, C Stockard, D Oelschlager, W Wan, U Manne, S Watts, and W Grizzle. 2009. Combined effects of formalin fixation and tissue processing on immunorecognition. *Biotech Histochem* 1-25.

Peckham, PH, and JS Knutson. 2005. Functional electrical stimulation for neuromuscular applications. *Annu Rev Biomed Eng* 7, 327-360.

Pickett, GE, M Campos-Benitez, JL Keller, and N Duggal. 2006. Epidemiology of traumatic spinal cord injury in Canada. *Spine (Phila Pa 1976)* 31, no. 7: 799-805.

Pikov, V, L Bullara, and DB McCreery. 2007. Intraspinal stimulation for bladder voiding in cats before and after chronic spinal cord injury. *J Neural Eng* 4, no. 4: 356-368.

Pileri, S, L Serra, and G Martinelli. 1980. The use of pronase enhances sensitivity of the PAP method in the detection of intracytoplasmic immunoglobulins. *Basic Appl Histochem* 24, no. 3: 203-207.

Pileri, SA, G Roncador, C Ceccarelli, M Piccioli, A Briskomatis, E Sabattini, S Ascani, D Santini, PP Piccaluga, O Leone, S Damiani, C Ercolessi, F Sandri, F Pieri, L Leoncini, and B Falini. 1997. Antigen retrieval techniques in immunohistochemistry: comparison of different methods. *J Pathol* 183, no. 1: 116-123.

Plath, N, O Ohana, B Dammermann, ML Errington, D Schmitz, C Gross, X Mao, A Engelsberg, C Mahlke, H Welzl, U Kobalz, A Stawrakakis, E Fernandez, R Waltereit, A Bick-Sander, E Therstappen, SF Cooke, V Blanquet, W Wurst, B Salmen, MR Bosl, HP Lipp, SG Grant, TV Bliss, DP Wolfer, and D Kuhl. 2006. Arc/Arg3.1 is essential for the consolidation of synaptic plasticity and memories. *Neuron* 52, no. 3: 437-444.

Prochazka, A, VK Mushahwar, and DB McCreery. 2001. Neural prostheses. *J Physiol* 533, no. Pt 1: 99-109.

Qiu, Z, and A Ghosh. 2008. A calcium-dependent switch in a CREST-BRG1 complex regulates activity-dependent gene expression. *Neuron* 60, no. 5: 775-787.

Raineteau, O, and ME Schwab. 2001. Plasticity of motor systems after incomplete spinal cord injury. *Nat Rev Neurosci* 2, no. 4: 263-273.

Rasouli, A, N Bhatia, P Dinh, K Cahill, S Suryadevara, and R Gupta. 2009. Resection of glial scar following spinal cord injury. *J Orthop Res* 27, no. 7: 931-936.

Renshaw, B. 1940. Activity in the simplest spinal reflex pathways. *J Neurophysiol*, 3(5):373-387.

Rexed, B. 1954. A cytoarchitectonic atlas of the spinal cord in the cat. *J Comp Neurol* 100, no. 2: 297-379.

Romanes, GJ. 1964. The Motor Pools of the Spinal Cord. *Prog Brain Res* 11, 93-119.

Rothstein, JD. 1996. Therapeutic horizons for amyotrophic lateral sclerosis. *Curr Opin Neurobiol* 6, no. 5: 679-687.

Rothwell, JC. 1987. Control of Human Voluntary Movement. Aspen Publication, Inc.

Sagar, SM, FR Sharp, and T Curran. 1988. Expression of c-fos protein in brain: metabolic mapping at the cellular level. *Science* 240, no. 4857: 1328-1331.

Saigal, R, C Renzi, and VK Mushahwar. 2004. Intraspinal microstimulation generates functional movements after spinal-cord injury. *IEEE Trans Neural Syst Rehabil Eng* 12, no. 4: 430-440.

Sharrard, WJ. 1964. The Segmental Innervation of the Lower Limb Muscles in Man. *Ann R Coll Surg Engl.* 35: 106-22.

- Sherrington, CS. 1898. Decerebrate Rigidity, and Reflex Coordination of Movements. *J Physiol* 22, no. 4: 319-332.
- Sherrington, CS. 1910. Flexion-reflex of the limb, crossed extension-reflex, and reflex stepping and standing. *J Physiol* 40, no. 1-2: 28-121.
- Shi, SR, RJ Cote, and CR Taylor. 1997. Antigen retrieval immunohistochemistry: past, present, and future. *J Histochem Cytochem* 45, no. 3: 327-343.
- Shi, SR, SA Imam, L Young, RJ Cote, and CR Taylor. 1995. Antigen retrieval immunohistochemistry under the influence of pH using monoclonal antibodies. *J Histochem Cytochem* 43, no. 2: 193-201.
- Shi, SR, ME Key, and KL Kalra. 1991. Antigen retrieval in formalin-fixed, paraffin-embedded tissues: an enhancement method for immunohistochemical staining based on microwave oven heating of tissue sections. *J Histochem Cytochem* 39, no. 6: 741-748.
- Shik, ML, and GN Orlovsky. 1976. Neurophysiology of locomotor automatism. *Physiol Rev* 56, no. 3: 465-501.
- Shuman, SL, JC Bresnahan, and MS Beattie. 1997. Apoptosis of microglia and oligodendrocytes after spinal cord contusion in rats. *J Neurosci Res* 50, no. 5: 798-808.
- Silver, J, and JH Miller. 2004. Regeneration beyond the glial scar. *Nat Rev Neurosci* 5, no. 2: 146-156.
- Singh, K, FJ Richmond, and GE Loeb. 2000. Recruitment properties of intramuscular and nerve-trunk stimulating electrodes. *IEEE Trans Rehabil Eng* 8, no. 3: 276-285.
- Smetana, R, L Juvin, R Dubuc, and S Alford. 2010. A parallel cholinergic brainstem pathway for enhancing locomotor drive. *Nat Neurosci* 13, no. 6: 731-738.
- Soffe, SR, A Roberts, and WC Li. 2009. Defining the excitatory neurons that drive the locomotor rhythm in a simple vertebrate: insights into the origin of reticulospinal control. *J Physiol* 587, no. Pt 20: 4829-4844.
- Tator, CH, and MG Fehlings. 1991. Review of the secondary injury theory of acute spinal cord trauma with emphasis on vascular mechanisms. *J Neurosurg* 75, no. 1: 15-26.

- Thuret, S, LD Moon, and FH Gage. 2006. Therapeutic interventions after spinal cord injury. *Nat Rev Neurosci* 7, no. 8: 628-643.
- Tikka, TM, and JE Koistinaho. 2001. Minocycline provides neuroprotection against N-methyl-D-aspartate neurotoxicity by inhibiting microglia. *J Immunol* 166, no. 12: 7527-7533.
- Tobias, CA, JS Shumsky, M Shibata, MH Tuszynski, I Fischer, A Tessler, and M Murray. 2003. Delayed grafting of BDNF and NT-3 producing fibroblasts into the injured spinal cord stimulates sprouting, partially rescues axotomized red nucleus neurons from loss and atrophy, and provides limited regeneration. *Exp Neurol* 184, no. 1: 97-113.
- Totoiu, MO, and HS Keirstead. 2005. Spinal cord injury is accompanied by chronic progressive demyelination. *J Comp Neurol* 486, no. 4: 373-383.
- University of Alabama at Birmingham. 2010. Spinal Cord Injury Facts and Figures at a Glance. National Spinal Cord Injury Statistical Center.
- van den Berg, ME, JM Castellote, I Mahillo-Fernandez, and J de Pedro-Cuesta. 2010. Incidence of Spinal Cord Injury Worldwide: A Systematic Review. *Neuroepidemiology* 34, no. 3: 184-192.
- Vanderhorst, VG, and G Holstege. 1997. Organization of lumbosacral motoneuronal cell groups innervating hindlimb, pelvic floor, and axial muscles in the cat. *J Comp Neurol* 382, no. 1: 46-76.
- Waller. 1850. Experiments on the Section of the Glossopharyngeal and Hypoglossal Nerves of the Frog, and Observations of the Alterations Produced Thereby in the Structure of Their Primitive Fibers. *Philosophical Transactions of the Royal Society of London* 140, 423-429.
- Wheeler, CA, and PH Peckham. 2009. Wireless wearable controller for upper-limb neuroprosthesis. *J Rehabil Res Dev* 46, no. 2: 243-256.
- Wolman, L. 1965. The Disturbance of Circulation in Traumatic Paraplegia in Acute and Late Stages: A Pathological Study. *Paraplegia* 2, 213-226.
- Wrathall, JR, YD Teng, and D Choiniere. 1996. Amelioration of functional deficits from spinal cord trauma with systemically administered NBQX, an antagonist of non-N-methyl-D-aspartate receptors. *Exp Neurol* 137, no. 1: 119-126.
- Wu, YP, CK Tan, and EA Ling. 1997. Expression of Fos-like immunoreactivity in the brain and spinal cord of rats following middle cerebral artery occlusion. *Exp Brain Res* 115, no. 1: 129-136.

Yakovenko, S, V Mushahwar, V VanderHorst, G Holstege, and A Prochazka. 2002. Spatiotemporal activation of lumbosacral motoneurons in the locomotor step cycle. *J Neurophysiol* 87, no. 3: 1542-1553.

Zompa, EA, LD Cain, AW Everhart, MP Moyer, and CE Hulsebosch. 1997. Transplant therapy: recovery of function after spinal cord injury. *J Neurotrauma* 14, no. 8: 479-506.